

Morse-Bott inequalities, Topology Change and Cobordisms to Nothing

Ignacio Ruiz

Instituto de Física Teórica UAM-CSIC, Universidad Autónoma de Madrid, Cantoblanco, 28049 Madrid, Spain

Departamento de Física Teórica, Universidad Autónoma de Madrid, Cantoblanco, 28049 Madrid, Spain

E-mail: ignacio.ruiz@uam.es

ABSTRACT: The Cobordism Conjecture predicts spacetime-ending configurations, such as Bubbles of Nothing (BoN), being commonplace. These correspond to vacuum decays in which the compactification manifold \mathcal{C}_n shrinks to a point, with the instability expanding at the speed of light and leaving nothing (not even spacetime) behind. Most constructions of BoN or cobordisms to nothing found in the literature feature simple instances of \mathcal{C}_n or singular cobordisms, which cannot be approached from the effective field theory. Assuming the solution mediating such decay to nothing is homeomorphic to a smooth description, we are able to go a step further, and obtain topological bounds on its homology for generic \mathcal{C}_n . Through the use of Morse-Bott theory we then translate this into information on the number and types of topology changes the compact manifold experiences as we move towards the tip of the bordism, as well as the location of possible cobordism defects. We illustrate our results with different detailed examples coming from String Theory. Furthermore, with this approach, we are able to study more complicated arrangements such as BoN collisions or intersection of End of the World branes.

Contents

1	Introduction	1
2	Dynamical bordisms into nothing	4
2.1	Bubbles of Nothing	4
2.2	End of the World Branes	8
3	Bordism Topology and Morse-Bott Inequalities	10
3.1	Bounding the topology of the bordism	11
3.2	Morse-Bott inequalities for manifolds with boundary	13
3.2.1	Some easy examples	17
3.3	Non-minimal bordisms and defects	18
4	Some more physical examples	20
4.1	Spheres with fluxes	20
4.2	Type IIB string theory on compact Riemann surfaces	22
4.3	An example of non-minimal bordism	30
4.4	A small step towards smooth bordisms for K3 compactifications.	32
5	Stories with more than one ending	34
5.1	<i>Seeing double</i> : Collisions of BoN's	34
5.2	<i>Going a bordism further</i> : Intersection of EotW branes	37
6	Conclusions and Outlook	41
A	Basics of Compact Riemann Surfaces	43
B	A quick overview of 1-cycle decay through tachyon condensation.	47

1 Introduction

One of the most surprising aspects of superstring theories is the prediction of $D = 10$ as the critical dimension ($D = 26$ for the bosonic string) of spacetime. In order to match the observed $d = 4$ of our universe, it is necessary to somehow get rid of the $n = D - d = 6$ extra directions. A straightforward way to do this is by *compactifying* them, in such a way that they take values on a compact n -dimensional manifold \mathcal{C}_n .

This procedure of *dimensional reduction* results in a low-energy d -dimensional effective field theory (EFT), which is valid for energies lower than the Kaluza-Klein scale. The choice of internal manifold, as well as other ingredients on it, such as fluxes or branes, will determine the field content of the EFT and its dynamics. The enormous set of different possible compactifications results in a large *landscape* of potential theories.

In the presence of such many vacua/low energy descriptions, the decay or transition into another is a general expectation, associated for example to different local minima in flux compactifications [1, 2], as well as topology changing transitions to a different compact manifold [3, 4], such as flops [5, 6] or conifolds [7, 8]. Generally speaking, topology changes are a generic expectation of Quantum Gravity, [9–14].

Another type of instability was shown by Witten [15], where the decay does not occur to a different vacuum, but rather to *nothing*, this is, to a configuration without spacetime. This construction, which will be reviewed in more detail in section 2.1, consists in a decay channel for a Minkowski vacuum with a single extra dimension compactified on a circle of radius R . A sphere of size R pops up, with spacetime ending smoothly on its surface, in such a way that its interior is non-accessible, with “nothing” (not even spacetime) being inside. The bubble expands with a velocity asymptotic to that of light, and as we approach its surface both the lower-dimensional curvature and the (normalized) scalar controlling the size of the circle blow up. This type of vacuum decay, dubbed *Bubble of Nothing* (BoN) has been generalized to other compactification manifolds and internal ingredients [16–37].

Bubbles of nothing and other spacetime ending configurations, such as Hořava-Witten walls [38, 39], might seem at first a curiosity without further implications. However, as shown in [40], this is not the case at all. The *Swampland program* [41–47], studies the set of constraints that an EFT with a consistent UV completion to Quantum Gravity must fulfill. One of the most established *Swampland Conjectures* is the **No Global Symmetries** conjecture [48–50], which postulates that there are no global charges in quantum gravity, so that any symmetry must be gauged or broken. A specific case of these global symmetries are *topological* ones. Since we expect some topology changes to be dynamically allowed in a theory of Quantum Gravity, this notion of topology change is better encapsulated by that of **cobordism class**. Two k -dimensional compact manifolds \mathcal{M}_k and \mathcal{N}_k are said to be *cobordant* if there exists a $(k+1)$ manifold \mathcal{B}_{k+1} such that $\partial\mathcal{B}_{k+1} = \mathcal{M}_k \sqcup \overline{\mathcal{N}_k}$. \mathcal{M}_k and \mathcal{N}_k are then said to be *(co)bordant* and \mathcal{B}_{k+1} is said to be a *bordism* between them. From a physical point, if compactifying our higher-dimensional theory on \mathcal{M}_k and \mathcal{N}_k results two distinct lower-energy descriptions, EFT_1 and EFT_2 , then traversing \mathcal{B}_{k+1} can be thought as crossing the domain wall relating

the two. This is illustrated in Figure 1.

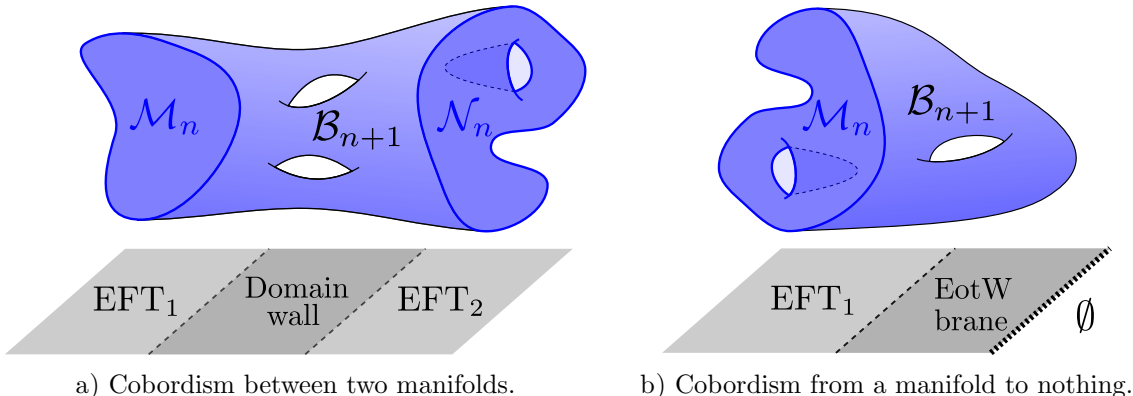


Figure 1. Sketch of different bordisms between n -manifolds. In subfigure 1a the bordism \mathcal{B}_{n+1} has as components of its boundary \mathcal{M}_n and \mathcal{N}_n , and can be interpreted as a domain wall between the two EFTs resulting from compactification on each of the manifolds. In subfigure 1b $\mathcal{M}_n = \partial\mathcal{B}_{n+1}$, the bordism connects the EFT to nothing, serving as a boundary of spacetime, which from the lower-dimensional perspective we will call *End of the World brane* in section 2.2.

Two compactifications that can be interpolated through a bordism or, in other words, for which there is a dynamically allowed topology change between them, are part of the same *cobordism class*. The topological charge associated to said classes is global rather than gauged [40], as one can take some spacetime \mathcal{X}_d , remove some submanifold $\mathcal{M}_k \subset \mathcal{X}_d$, and glue along it some other \mathcal{N}_k in the same cobordism class as \mathcal{M}_k . The resulting spacetime is cobordant to the original one, but far from the region where we have changed the local topology, both look the same, and the topology of this defect introduced cannot be inferred. Per the No Global Symmetries conjecture, this cannot occur in a gravitational theory with a consistent UV completion. The solution to this problem is this topological charge being trivial, or in other words, by requiring that our compactification manifold must be the boundary of an appropriate bordism, $\mathcal{M}_n = \partial\mathcal{B}_{n+1}$. This is known as the **Swampland Cobordism Conjecture** [40].

While the above might seem like a pretty abstract discussion about compactifications of QG, it has a radical implication: since then all compactifications of QG, say string theory, must be in the same cobordism class, they should be connected through some domain wall to **nothing**, this is, have spacetime ending boundary such as Witten’s BoN.¹ From the bordism point of view, this corresponds with the internal manifold smoothly capping off to a point, after which spacetime ends. If more stringy, singular objects are allowed, such as O-planes, then this is not necessarily the case, as the compact manifold itself can have boundaries, which themselves serve as domain walls to nothing. More exotic defects might be needed to kill cobordism classes to the trivial one, which has result in the prediction of new, often

¹As discussed in section 2.1, an extra requirement will be that such decay is dynamically allowed, this being a general expectation in non-SUSY compactifications.

non-supersymmetric objects [40, 51, 52], but their inclusion in the bordism is likely to result in singular solutions.

Controlled solutions, solving the equations of motion, and describing explicit bordisms to nothing are rare in the literature, and usually correspond with simple compactification manifolds such as spheres or tori [16–29, 31–37]. The few explicit examples for more complicated cases without the need of stringy defects are quite involved [30]. Smooth solutions are crucial from the phenomenological point of view, as they can be approached from the supergravity approximation. Furthermore, their nucleation rate (per unit volume) as a decay channel for the initial configuration will be dominant, and can be computed semiclassically $\Gamma_{\text{BoN}}/\text{Vol}_d \sim e^{\Delta S^{(E)}}$ [53], with $\Delta S^{(E)}$ the difference in Euclidean action between the initial vacua and the BoN solution. Singular bordisms will have divergent terms in their Euclidean action, and thus will be suppressed.

The **goal of our paper** is to take a *first step* in the construction of *smooth* bordisms into nothing, as well as those which might have singular terms, but for which nonetheless \mathcal{B}_{n+1} is *homeomorphic* to a smooth manifold. We will call said bordisms *smoothable*. We will obtain bounds in the topology of \mathcal{B}_{n+1} from that of $\mathcal{C}_n = \partial\mathcal{B}_{n+1}$, and understand how this changes as we move along the bordism. Precisely for compact manifolds \mathcal{C}_n with an involved internal topology, featuring different internal cycles of various dimensions, these smooth bordisms to nothing \mathcal{B}_{n+1} cannot be the complete manifold \mathcal{C}_n as a whole smoothly shrinking to a point², but rather has a more involved structure, with the different internal cycles shrinking before the final tip into nothing. This corresponds with intermediate topology changes, which will be associated with a series of domain walls before, or “coating”, the final boundary to nothing. Our approach will be able to give us information about the internal structure of both Bubbles of Nothing that dynamically nucleate and, as well as more general fixed End of the World branes in interpolating from our EFT theory into nothing.

As it is easy to imagine, explicit solutions featuring these intermediate topology changes are quite involved. We will not attempt to write those, but simply obtain qualitative information about the structure of smooth(able) bordisms into nothing. The tool for this will be **Morse theory**, interpreting the bordism direction in \mathcal{B}_{n+1} as our Morse function, whose critical points we will understand as the loci where the internal topology changes. As a matter of fact, Morse theory is nothing new in high energy theoretical physics, with the seminal work by Witten [54] giving a supersymmetric system interpretation, which allowed him to derive a version of the so-called **Morse inequalities** we will use in this work, relating the set of critical points of a function with the topology of the manifold it is defined over.³ Our

²One could simply consider the cone $C(\mathcal{C}_n) = (\mathcal{C}_n \times [0, 1]) / \sim$, with $(x, 1) \sim (y, 1)$ for all $x, y \in \mathcal{C}_n$, but it can be shown that $C(\mathcal{C}_n)$ is not a topological manifold unless $H_k(\mathcal{C}_n, \mathbb{Z}) \simeq \mathbb{Z}$ for $k = 0, n$ and 0 otherwise, i.e., \mathcal{C}_n is a homology sphere.

³Morse theory had already been considered in the literature [55–60] for spacetime topology changes. Unlike in our case, in which these changes occur as we move spatially towards the end of our spacetime (be it the tip of the BoN or more generally the End of the World brane, see section 2), there the topology changes occur in the time direction, with the Lorentzian metric vanishing precisely at the critical points of the Morse function with which it is constructed. The similarities between our approach and theirs end here, as we will not need

work goes in line with recent approaches trying to infer local information of the EFT from topological global properties [61]. We will also be able to use the Morse theory tools to obtain qualitative properties of configurations where more than one bordism to nothing is present.

The structure of the paper is as follows. In section 2 we review basic concepts of Bubbles of Nothing and End of the World branes, using Witten’s BoN as the canonical example. In section 3 we introduce the necessary algebraic topology and Morse theory tools needed to obtain information about the topology of the bordism \mathcal{B}_{n+1} from the compact manifold \mathcal{C}_n , as well as the possible intermediate topology changes. We use these results in section 4 on some compactification examples, showcasing the changes in the low-energy EFT, while in section 5 we consider the possibility that different bordisms to nothing come into play simultaneously, and how Morse theory can help us obtain information about these configurations. Finally, in section 6 we conclude by summarizing our results and highlighting possible future directions.

2 Dynamical bordisms into nothing

We will begin with a short review Witten’s **Bubble of Nothing**, as well as its generalization to other compactification manifolds and how the lower EFT “sees” this spacetime boundaries. We will then use it as a starting points for generalizations to more involved compact topologies.

2.1 Bubbles of Nothing

The simplest (and coincidentally first found to appear in the literature) dynamical bordism into nothing is Witten’s **Bubble of Nothing** [15], presented here for an arbitrary number of spacetime (non-compact) dimensions. To study this non-perturbative instability of Kaluza-Klein vacuum, consider a circle compactification to a d -dimensional Minkowski, with global spacetime $X_{d+1} = \mathbb{R}^{1,d} \times \mathbb{S}^1$, with \mathbb{S}^1 of radius R . This instability can be constructed from a Schwarzschild instanton $\hat{\mathcal{S}}_{d+1}$ in the Euclidean continuation of our spacetime, $X_{d+1}^{(E)} = \mathbb{R}^{d+1} \times \mathbb{S}^1$, which will have metric

$$ds_{d+1}^2 = r^2 d\Omega_{d-1}^2 + \frac{dr^2}{1 - \left(\frac{R}{r}\right)^{d-2}} + R^2 \left[1 - \left(\frac{R}{r}\right)^{d-2} \right] d\theta^2, \quad \text{with } \theta \in [0, 2\pi), \quad (2.1)$$

where R is the nucleation radius of the instanton. It is easy to see that for $r \gg R$, $ds_{d+1}^2 \approx dr^2 + r^2 d\Omega_{d-1}^2 + R d\theta^2$ and the space locally looks like $X_{d+1}^{(E)} = \mathbb{R}^{d+1} \times \mathbb{S}^1$. Expanding $d\Omega_{d-1}^2 = d\lambda^2 + \sin^2 \lambda d\Omega_{d-2}^2$, with $\lambda \in [0, \pi)$, we can go back to Lorentzian signature, by identifying $t = 0$ with $\lambda \equiv \frac{\pi}{2}$, and Wick-rotating $\lambda \rightarrow \frac{\pi}{2} + i\tau$, under which

$$ds_{d+1}^2 = -r^2 d\tau^2 + \frac{dr^2}{1 - \left(\frac{R}{r}\right)^{d-2}} + r^2 \cosh^2 \tau d\Omega_{d-2}^2 + R^2 \left[1 - \left(\frac{R}{r}\right)^{d-2} \right] d\theta^2, \quad (2.2)$$

to worry about problems of causality, the main focus of attention of said references.

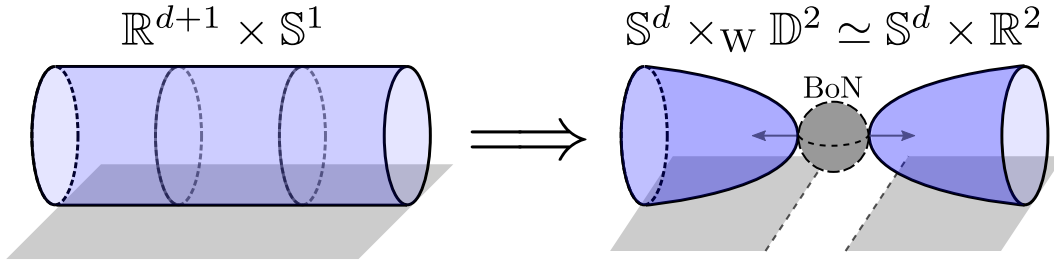


Figure 2. Euclidean sketch of the d -dimensional version of Witten’s BoN (together with the Wick rotated KK Minkowski vacuum), with the macroscopic dimensions being the horizontal gray direction depicted in gray. Notice that far from the BoN surface, both spaces are locally identical.

which in the $r \gg R$ limit, and after redefining $x = r \cosh \tau$ and $t = r \sinh \tau$ (see that precisely $t = 0$ for $\lambda = \frac{\pi}{2}$), looks locally like X_{d+1} ,

$$ds_{d+1}^2 \approx -dt^2 + dx^2 + x^2 d\Omega_{d-2}^2 + R^2 d\theta^2 . \quad (2.3)$$

However, precisely the fascinating observation made in [15] is that the new time and radial coordinates t and x do not cover the full original X_{d+1} , only those parts with $x^2 - t^2 = r^2 \geq R^2$, with $r = R$ corresponding to the wall of the *bubble* at the time of nucleation $t = 0$. The “inside” of the $x^2 - t^2 = R^2$ hyperboloid is now removed from spacetime. The size of the extra dimension

$$\hat{R}(r) = R \sqrt{1 - \left(\frac{R}{r}\right)^{d-2}} \quad (2.4)$$

shrinks as we approach the bubble wall, $x_{\text{BoN}} = \sqrt{R^2 + t^2}$, which asymptotically expands at the speed of light. In order to avoid a conical singularity at x_{BoN} the condition $R = R$ (i.e., the bubble nucleates at the KK scale) is required. A smooth solution is required in order to avoid curvature singularities and non-geodesically complete spacetimes, though as we will see in sections 3 and 3.3 for our analysis we will only require that the BoN solution has a topological manifold structure, regardless of possible singularities of stringy origin. As shown in Figure 2, the Euclidean solution has global topology $\hat{\mathcal{S}}_{d+1} \simeq \mathbb{S}^{d-1} \times_{\text{W}} \mathbb{D}^2 \simeq \mathbb{S}^{d-1} \times \mathbb{R}^2$, where \times_{W} is a warped product and $\mathbb{D}^n = \{x \in \mathbb{R}^n : \|x\| \leq 1\}$ is the n -disc, with indeed $\partial \mathbb{D}^2 = \mathbb{S}^1$.

Already in the original appearance of Witten’s BoN [15] a possible topological obstruction to the KK vacuum decay was postulated in the presence of fermions. Being $\hat{\mathcal{S}}_{d+1}$ simply connected, there is a unique spinor structure, which here it is set by the asymptotics far from the bubble wall, where space locally looks like $\mathbb{R}^d \times \mathbb{S}^1$. Under a 2π rotation along \mathbb{S}^1 , spinors can have either symmetric or antisymmetric boundary conditions. However, if we want to be able to extend the solution to the complete $\hat{\mathcal{S}}_{d-1}$, the spin structure must be extended to the whole \mathbb{D}^2 . Since this is contractible, only antiperiodic spin structure makes sense for the BoN solution to exist. Since this accounts for non-covariantly constant spinors, SUSY

must be broken either in the higher-dimensional theory or explicitly through the imposition of Scherk-Schwarz boundary conditions [62–64] when compactifying.

As for whether the vacuum decay is energetically allowed, the ADM mass computation shows (2.2) to have 0 energy (same as $X_{d+1} = \mathbb{R}^{1,d-1} \times \mathbb{S}^1$). The *Positive Energy Theorem* [65, 66], i.e., that every non-flat solution of Einstein’s equations asymptoting to Minkowski has positive energy (thus semiclassically preventing Minkowski decay) does not apply here when antiperiodic boundary conditions are used in \mathbb{S}^1 , as the proof of the theorem relays on the existence of covariantly constant spinors. The decay rate (per unit volume per unit time) can be computed to be $\Gamma \sim \exp \left\{ -2\pi^{d/2} \Gamma(\frac{d}{2})^{-1} (\mathbb{R} M_{\text{Pl},d})^{d-2} \right\}$, with all contributions coming from the Gibbons–Hawking–York term (the BoN solution being Ricci-flat) and having $\Gamma \rightarrow 0$ for large radius.

As mentioned above, the topology of the Euclidean instanton $\hat{\mathcal{S}}_{d+1}$ (2.1) is not $\mathbb{R}^{d+1} \times \mathbb{S}^1$, but rather $\mathbb{S}^{d-1} \times_{\mathbb{W}} \mathbb{D}^2$. As explained in [30], this can be made more explicit by rewriting the Euclidean solution 2.1 as

$$ds_{d+1}^2 = \mathcal{W}(\rho)^2 d\Omega_{d-1}^2 + d\rho^2 + \hat{\mathbb{R}}(\rho)^2 d\theta^2, \quad \text{with } \rho \in [0, \infty), \theta \in [0, 2\pi), \quad (2.5)$$

where $\mathcal{W}(\rho)$ is some warping function.⁴ Precisely for constant angle \mathbb{S}^{d-1} direction in (2.5) the metric simplifies to

$$ds_2^2 = d\rho^2 + \hat{\mathbb{R}}(\rho)^2 d\theta^2, \quad (2.7)$$

which is precisely the $\mathbb{R}^2 \simeq \mathbb{D}^2$ metric in polar coordinates, with the $\rho \rightarrow \infty$ limit resulting in $\hat{\mathbb{R}}^2 d\theta^2 = \mathbb{R}^2 d\theta^2$ metric for the compact \mathbb{S}^1 in the original spacetime.

While Witten’s Bubble of Nothing is in many aspects very simple, it serves as a first step from which we can generalize to more involved bubbles of nothing. In general, starting with a $X_{d+n} = \mathbb{R}^{1,d-1} \times \mathcal{C}_n$ Minkowski compactification, the associated Euclidean instanton mediating the bubble of nothing will have $\hat{\mathcal{S}}_{d+n} \simeq \mathbb{S}^{d-1} \times_{\mathbb{W}} \mathcal{B}_{n+1}$ topology, with \mathcal{B}_{n+1} the bordism from \mathcal{C}_n to nothing, i.e., $\partial \mathcal{B}_{n+1} = \mathcal{C}_n$. In the language of (2.5), this results in the following $SO(d-1)$ symmetric ansatz [30] for the Euclidean solution:

$$ds_{d+n}^2 = W(y)^2 \mathbb{R}^2 d\Omega_{d-1}^2 + h_{\alpha\beta}^{\mathcal{B}}(y) dy^\alpha dy^\beta, \quad (2.8)$$

where \mathbb{R} is the nucleation radius and $h_{\alpha\beta}^{\mathcal{B}}$ is the metric of the bordism \mathcal{B}_{n+1} , parameterized by $\{y^\alpha\}_{\alpha=1}^{n+1}$. Denoting the radial direction from the bubble as $\rho(y) = W(y)\mathbb{R} \in [0, \infty)$, far

⁴The radial directions are related by $r = \mathbb{R}W(\rho)$, with the bubble located at $\rho = 0$ and the warping fulfilling

$$W'(\rho) = \mathbb{R}^{-1} \sqrt{1 - W(\rho)^{-(d-2)}}, \quad W(0) = 1 \iff {}_2F_1 \left(\frac{1}{2}, \frac{1}{2-d}, \frac{3-d}{2-d} W(\rho)^{2-d} \right) W(\rho) = \frac{\rho}{\mathbb{R}}, \quad (2.6)$$

which for large ρ asymptotics to $W(\rho) \approx \frac{\rho}{\mathbb{R}}$ and $r \approx \rho$, as expected.

away $\rho \rightarrow \infty$ we can rewrite (2.8) as

$$ds_{d+n}^2 \approx \rho^2 d\Omega_{d-1}^2 + \underbrace{d\rho^2 + h_{\bar{\alpha}\bar{\beta}}^{\mathcal{C}} dy^{\bar{\alpha}} dy^{\bar{\beta}}}_{h_{\bar{\alpha}\bar{\beta}}^{\mathcal{B}}(y) dy^{\bar{\alpha}} dy^{\bar{\beta}}}, \quad (2.9)$$

where now we can separate the bordism coordinates into the radial direction and the internal parametrization of the compact \mathcal{C} , $\{y^\alpha\}_{\alpha=1}^{n+1} \rightarrow \{\rho\} \cup \{y^{\bar{\alpha}}\}_{\bar{\alpha}=1}^n$, and $h_{\bar{\alpha}\bar{\beta}}^{\mathcal{C}}$ the asymptotic metric of \mathcal{C}_n in X_{d+n} , independent of the radius ρ . This way, far from the bubble wall, the solution locally looks like the initial compactification. The Wick rotation back to Minkowski can be performed in the same way as in Witten's BoN, with no additional difficulties from the more complicated compact \mathcal{C}_n , as the Wick rotation is performed on the sphere \mathbb{S}^{d-1} to a hyperboloid.

As explained earlier in this section, for Witten's BoN to exist, it was crucial that the compactification manifold \mathbb{S}^1 had antiperiodic (i.e., SUSY-breaking) boundary conditions. Furthermore, one would have to argue that the process is not kinematically obstructed and has a finite decay rate. This translates to more general BoN decays through the following two conditions [30]:

- **Topological Condition:** This first requirement translates in all compactification manifolds belonging to the trivial cobordism class. When considering \mathcal{M}_k and \mathcal{N}_k to be \mathfrak{g} -manifolds, with \mathfrak{g} some appropriate structure, then the \mathfrak{g} -bordism is defined such that \mathcal{B}_{k+1} is also a \mathfrak{g} -manifold, and the associated \mathfrak{g} -structure restricted to each of $\partial\mathcal{B}_{k+1}$ components corresponds to that of \mathcal{M}_k and \mathcal{N}_k . The notion of cobordism defines an equivalence relation between compact manifolds, and $[\mathcal{M}_k] = [\mathcal{N}_k]$. We denote the set of cobordism classes by $\Omega_k^{\mathfrak{g}}$, which can be shown to have a Abelian group structure, such that $[\mathcal{M}] + [\mathcal{N}] = [\mathcal{M} \sqcup \overline{\mathcal{N}}]$. Through the **Swampland Cobordism Conjecture** this condition is automatically satisfied by requiring $\Omega_{\bullet}^{\text{QG}} = 0$. As the complete, non-perturbative description of quantum gravity is not yet known, we will approximate this QG structure by simpler \mathfrak{g} whose cobordism groups are better understood. In section 3.3 we comment on the necessary defects that might be required to trivialize non-zero cobordism groups, $\Omega_k^{\mathfrak{g}} \neq 0 \rightarrow \Omega_k^{\mathfrak{g}+\text{defects}} = 0$.

Translating this topological condition to Witten's BoN, the circle with antiperiodic boundary conditions \mathbb{S}_a^1 belongs to the trivial class of $\Omega_1^{\text{Spin}} \simeq \mathbb{Z}_2$ [67], with the second class given by the periodic circle \mathbb{S}_p^1 . As on principle the later is an allowed compactification manifold, from the Cobordism Conjecture point of view, there must exist either UV defects that can change the spin structure [40, 68], or either the QG structure $\mathfrak{g} = \text{Spin}$ must be refined to $\hat{\mathfrak{g}}$ such that $\Omega_1^{\hat{\mathfrak{g}}} = 0$, for instance to $\Omega_1^{\text{Spin}^c} = 0$, see [69].

- **Dynamical Condition:** The Positive Energy Theorem (PET) [66, 70, 71] states that the ADM mass of asymptotically $\mathcal{M}_{d+n} \simeq \mathbb{R}^{1,d-1} \times \mathcal{C}_n$ (with \mathcal{C}_n compact) spacetimes is bounded from below by 0, with the only spacetime saturating the inequality being

precisely $\mathbb{R}^{1,d-1} \times \mathcal{C}_n$. This prevents any bubble nucleation, since any BoN spacetime will have more energy, and as such the decay will be obstructed. PET relies on the assumption that **(1)** \mathcal{M}_{d+n} admits an asymptotically covariantly constant spinor (always the case when SUSY is preserved) and **(2)** the *Dominant Energy Condition* (DEC), i.e., $-g_{BC}T^{AB}k^C$ is causal and future-pointing for all k^C causal and future-pointing vectors, holds. While **(1)** is a topological condition which depends on the global structure of spacetime, **(2)** depends on the matter and higher-derivative ingredients of our EFT. There is a rich literature on how any of these two conditions can be broken, specially **(2)** [30, 53, 72], so that the PET does not apply.

As for the most part of this paper we will be interested in the qualitative properties of our bordisms to nothing, we will assume that the above conditions hold and thus such bordism can be realizable. In general, the difficulty in building the appropriate BoN solution for a given compactification stems from finding the appropriate bordism solution $h_{\alpha\beta}^{\mathcal{B}}$ to the equations of motion, as well as including the appropriate defects to kill the bordism group $\Omega_n^{\mathcal{G}}$. While much effort has been done in the past years in finding explicit BoN constructions [15–37] (see also [73–77] for related problems and techniques), most of the solutions feature relatively simple topologies along the bordism direction. One can imagine that as the topology of the internal manifold \mathcal{C}_n becomes more involved, so will that of the bordism \mathcal{B}_{n+1} . In section 3 we will see that indeed we can obtain plenty of information about these simply from the topology of \mathcal{C}_n .

2.2 End of the World Branes

In the above section, we have kept a higher-dimensional description. One can wonder now how Witten’s BoN looks from the d -dimensional description once the internal coordinate is integrated out. Dimensionally reducing (2.1) down to d -dimensions (see [78] for more details) results in the following metric in the (Euclidean) Einstein frame:

$$ds_d^2 = \left(\frac{\hat{R}(r)}{R} \right)^{2\frac{3-d}{d-2}} dr^2 + \left(\frac{\hat{R}(r)}{R} \right)^{\frac{2}{d-2}} d\Omega_{d-1}^2, \quad (2.10)$$

with $\hat{R}(r)$ as defined in (2.4), and the $(d+1, d+1)$ component of the higher dimensional metric being promoted to a (massless) scalar, which can be canonically normalized to the following radion profile

$$\varrho(r) = -\sqrt{\frac{d-1}{d-2}} \log \left[\frac{\hat{R}(r)}{R} \right], \quad (2.11)$$

with the overall sign being only a matter of convention. Note that as we approach the BoN tip $r \rightarrow R$, $\hat{R}(r) \rightarrow 0$ and the radion blows up, $\varrho \rightarrow \infty$. As the compact manifold is flat, there is no induced curvature potential to the d -dimensional action. Note that, even though,

being a solution of Einstein's equations in vacuum, (2.1) is Ricci-flat,⁵ this is no longer the case once we compactify, with the Ricci scalar of (2.10) given by

$$\mathcal{R} = \frac{(d-2)(d-1)}{4R^2} \left(\frac{R}{r}\right)^{2(d-1)} \left(\frac{\hat{R}(r)}{R}\right)^{-2\frac{d-1}{d-2}}, \quad (2.12)$$

which blows up as we approach $r \rightarrow R$. In terms of the actual traversed physical distance in the radial direction, this can be computed from (2.10) to be

$$\Delta r = \frac{2(d-2)^2 R}{d-1} \left(\frac{\hat{R}(r)}{R}\right)^{\frac{d-1}{d-2}}, \quad (2.13)$$

which means that the bubble wall $r = R$ ($\Delta r = 0$) is at finite spacetime distance. Furthermore, as we approach said locus, both the radion and Ricci scalar scale as

$$\varrho \sim -\sqrt{\frac{d-2}{d-1}} \log\left(\frac{\Delta r}{R}\right) \rightarrow \infty, \quad \mathcal{R} \sim e^{2\sqrt{\frac{d-1}{d-2}}\varrho} \sim \frac{1}{\Delta r^2} \rightarrow \infty. \quad (2.14)$$

As expected from infinite distance regions in moduli space being proven, $\varrho \rightarrow \infty$, there is a break-down of the lower-dimensional EFT from the blowing-up spacetime curvature $\mathcal{R} \rightarrow \infty$.

The above behaviors are not unique to Witten's BoN, but rather universal features of the close distance behavior of *End of the World branes*. As introduced in [78], general solutions to d -dimensional Einstein gravity coupled to a canonically normalized scalar ϕ (generalizable to more scalars and non-canonical metrics) and a potential $V(\phi)$, in the presence of a real codimension-1 boundary (the End of the World Brane), feature the following scalings

$$\phi(\Delta r) \sim -\frac{2}{\delta} \log \Delta r, \quad |\mathcal{R}| \sim \Delta r^{-2} \sim e^{\delta\phi}. \quad (2.15)$$

Both scalings are given in terms of a *critical exponent* δ given by

$$\delta = 2\sqrt{\frac{d-1}{d-2}(1-a)}, \quad (2.16)$$

where a is given by

$$a = \frac{V(\phi)}{V(\phi) - \frac{1}{2}(\partial_{\Delta r}\phi)^2} \leq 1, \quad (2.17)$$

as from the e.o.m. $\frac{1}{2}(\partial_{\Delta r}\phi)^2 \geq V(\phi)$. Note that for Witten's BoN there is no potential and as such $a = 0$, with $\delta = 2\sqrt{\frac{d-1}{d-2}}$, see (2.14). For $a < 1$ equations of motion result in a scalar potential of the form $V(\phi) \sim V_0 e^{\delta\phi}$, with the potential (if present) blowing up at the EotW brane. Solutions with $a = 1$ are more exotic, as they allow for sub-exponential dependence,

⁵The Riemann tensor, as well as some curvature invariants derived from it, are not null for (2.1), though they remain small if R is large in $M_{\text{Pl},5}$ units, which in turn results in a smaller decay rate.

with expressions (2.15) not applying.

The example above features a smooth bordism into nothing, with the internal cycle quietly shrinking to a point. In [79] a general analysis of non-smooth bordisms is presented, with the angular defect at the tip of the bordism being related to the tension of the EotW brane, [80, 81].

The EotW brane description has been extensively studied from the dynamical cobordism point of view [79, 82–101], and while there is not a one-to-one correspondence between the critical exponent δ and the UV resolution of the EotW brane, some steps have been performed towards a classification [102]. While in the cobordisms to nothing from Witten’s BoN and other instances in the literature (see [78] for some simple examples) the scalar ϕ denotes the volume of the internal manifold, which shrinks to nothing, as we will see in section 4, more involved bordisms have several (canonically normalized) moduli going to infinite distance as we radially traverse our bordism towards its “boundary to nothing”. These scalars need not blow up at the same locus, with the EotW brane being “thick” and having some internal structure, precisely corresponding with the different topology changes which we will describe shortly in 3. This is in no way surprising, as both the EFT description breaking can be seen from the scalars traveling to infinite distance in moduli space, or equivalently from the change in the compactification manifold topology which results in a different lower-dimensional EFT.

3 Bordism Topology and Morse-Bott Inequalities

In the general introduction to BoN and EotW branes, the bordism \mathcal{B}_{n+1} from the compact manifold \mathcal{C}_n to nothing was extensively used. As discussed in sections 1 and 2, a necessary condition for \mathcal{B}_{n+1} to exist was that $\Omega_n^g = 0$, with $\partial\mathcal{B}_{n+1} = \mathcal{C}_n$ and the structure \mathfrak{g} extending from \mathcal{C}_n to \mathcal{B}_{n+1} . However, even when such bordism exists, it will not be unique.

As an illustrative example, take \mathbb{S}^1 together with the oriented bordism. As $\Omega_1^{SO} = 0$ [103], there is no obstruction from this side, and actually it is straightforward that $\mathbb{S}^1 = \partial\mathbb{D}^2$. However, more generally the circle is the boundary of any genus- g Riemann surface Σ_g with a disk removed, $\mathbb{S}^1 = \partial(\Sigma_g - \mathbb{D}^2)$, with $\mathbb{D}^2 = \mathbb{S}^2 - \mathbb{D}^2$, see Figure 3. More in general, given some compact $\mathcal{C}_n = \partial\mathcal{B}_{n+1}$, one can always define $\mathcal{B}'_{n+1} = \mathcal{B}_{n+1} \# \mathcal{Y}_{n+1}$, with some appropriate \mathcal{Y}_{n+1} not homeomorphic to \mathbb{S}^{n+1} and to which the structure \mathfrak{g} also extends. This way \mathcal{B}'_{n+1} and \mathcal{B}_{n+1} will be topologically distinct while both having \mathcal{C}_n as boundary. This means that (at least only from topological data), both $\mathbb{S}^{d-1} \times_{\mathbb{W}} \mathcal{B}_{n+1}$ and $\mathbb{S}^{d-1} \times_{\mathbb{W}} \mathcal{B}'_{n+1}$ are two different topologies for BoN decay channels of $\mathbb{R}^d \times \mathcal{C}_n$, both looking the same far from the bubble wall/EotW brane.

Intuitively, as we move along the radial direction ρ towards the bubble wall $\rho = 0$, the difference between the two constructions lies in the *necessary* topology changes

$$\mathcal{C}_n = \mathcal{C}_n^{(0)} \rightarrow \mathcal{C}_n^{(1)} \rightarrow \dots \rightarrow \mathcal{C}_n^{(m)} = \emptyset \tag{3.1}$$

in the local compactification manifold, given by the section or fiber of \mathcal{B}_{n+1} . The local theory undergoes in the compact manifold, with different internal cycles opening and closing, until we reach the boundary to nothing. As an illustration, return to the bordisms of the circle $\mathbb{S}^1 = \partial\mathbb{D}^2 = \partial(\mathbb{T}^2 - \mathbb{D}^2)$, depicted in Figure 3. While in the former case the minimal topology change is $\mathbb{S}^1 \rightarrow \emptyset$ as the circle shrinks to nothing (Witten’s BoN), for the later one undergoes $\mathbb{S}^1 \rightarrow \mathbb{S}^1 \sqcup \mathbb{S}^1 \rightarrow \mathbb{S}^1 \rightarrow \emptyset$, which involves two extra topology changes.

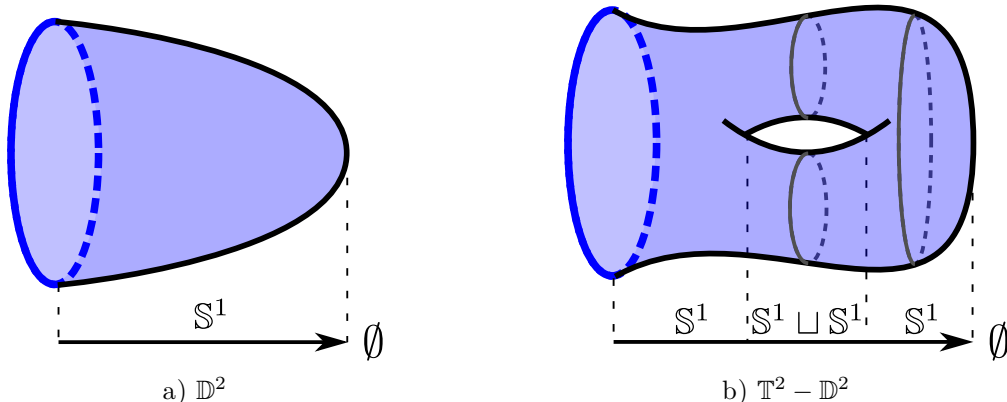


Figure 3. Two instances of oriented bordism from \mathbb{S}^1 to nothing, with the associated minimal topology changes in each.

As a result, the dimensional reduction from the higher-dimensional description results in distinct low-energy EFTs, such that before the final bordism into “nothing” one would encounter a series of domain walls separating the different topologies. Whilst from the EFT point of view the EotW brane and the accompanying diverging scalar correspond to the domain wall associated with the first topology change we encounter, there can be a “more complicated” structure “inside” such brane, dressed by said first domain wall.

Of the two bordisms depicted in Figure 3, we know that the one that actually describes a known “dynamical” process is that of Figure 3a, Witten’s BoN, for which there are no intermediate topology changes. We will encounter that of Figure 3b again in section 3.3 in the context of more complicated bordism groups. The question that naturally arises now is whether one can always go to nothing in a single step, or if intermediate topology changes are required once the internal manifold \mathcal{C}_n is complicated enough. To answer this, we will need to obtain information about (1) the topology of the possible bordisms \mathcal{B}_{n+1} and (2) how the radial direction ρ interpolates the bordism \mathcal{B}_{n+1} on its way to \emptyset , and how this translates into the *necessary topology changes*.

3.1 Bounding the topology of the bordism

The first of the two above tasks is the most straightforward, as it will only involve some careful manipulation of long exact sequences. For simplicity, we will restrict to bordisms

admitting a continuous deformation to a smooth topological manifold⁶. Consider for this a $(n + 1)$ -dimensional smooth manifold \mathcal{B}_{n+1} with boundary $\mathcal{C}_n = \partial\mathcal{B}_{n+1} \neq \emptyset$. For further simplicity we will assume \mathcal{B}_{n+1} to be orientable.

We start applying by applying the snake lemma, which results in the following long exact sequence:

$$\cdots \rightarrow H_k(\mathcal{C}_n; \mathbb{Z}) \rightarrow H_k(\mathcal{B}_{n+1}; \mathbb{Z}) \rightarrow H_k(\mathcal{B}_{n+1}, \mathcal{C}_n; \mathbb{Z}) \rightarrow H_{k-1}(\mathcal{C}_n; \mathbb{Z}) \rightarrow \cdots, \quad (3.2)$$

where $H_k(\mathcal{X}; \mathbb{Z})$ is the k -th homology group with integer coefficients and $H_k(\mathcal{X}, \mathcal{Y}; \mathbb{Z})$, with $\mathcal{Y} \subseteq \mathcal{X}$, is the relative homology group, whose elements are represented the n -chains α of \mathcal{X} whose boundary $\partial\alpha$ is a $(n - 1)$ -chain of $\mathcal{Y} \subseteq \mathcal{X}$. Applying now Lefschetz duality, $H^k(\mathcal{B}_{n+1}, \mathcal{C}_n; \mathbb{Z}) \simeq H_{n+1-k}(\mathcal{B}_{n+1}; \mathbb{Z})$, we can rewrite (3.2) as

$$\cdots \rightarrow H^{n-k}(\mathcal{B}_{n+1}; \mathbb{Z}) \simeq H_{k+1}(\mathcal{B}_{n+1}, \mathcal{C}_n; \mathbb{Z}) \rightarrow H_k(\mathcal{C}_n; \mathbb{Z}) \rightarrow H_k(\mathcal{B}_{n+1}; \mathbb{Z}) \rightarrow \cdots. \quad (3.3)$$

On the other hand, given some manifold \mathcal{M} , we can separate the torsion and free parts of its homology groups,

$$T_k(\mathcal{M}) := \tau H_k(\mathcal{M}; \mathbb{Z}), \quad fH_k(\mathcal{M}; \mathbb{Z}) := H_k(\mathcal{M}; \mathbb{Z})/T_k(\mathcal{M}), \quad (3.4)$$

which for orientable n -manifolds without boundary, such as \mathcal{C}_n , obey

$$fH_k(\mathcal{M}; \mathbb{Z}) \simeq fH_{n-k}(\mathcal{M}; \mathbb{Z}), \quad T_k(\mathcal{M}) \simeq T_{n-k-1}(\mathcal{M}), \quad (3.5)$$

note the extra -1 in the torsion part. Now, for integral (co)homology, the Universal Coefficient Theorem states that

$$H_k(\mathcal{M}; \mathbb{Z}) \simeq \mathbb{Z}^{b_k(\mathcal{M})} \otimes T_k(\mathcal{M}) \iff H^k(\mathcal{M}; \mathbb{Z}) \simeq \mathbb{Z}^{b_k(\mathcal{M})} \otimes T_{k-1}(\mathcal{M}), \quad (3.6)$$

where $b_k(\mathcal{M})$ are the (integral) Betti numbers of \mathcal{M} . This allows us to rewrite (3.3) as

$$\cdots \rightarrow \mathbb{Z}^{b_{n-k}(\mathcal{B}_{n+1})} \otimes T_{n-k-1}(\mathcal{B}_{n+1}) \rightarrow \mathbb{Z}^{b_k(\mathcal{C}_n)} \otimes T_k(\mathcal{C}_n) \rightarrow \mathbb{Z}^{b_k(\mathcal{B}_{n+1})} \otimes T_k(\mathcal{B}_{n+1}) \rightarrow \cdots. \quad (3.7)$$

Denoting $t_k(\mathcal{M}) = \text{rank } T_k(\mathcal{M})$, we can conclude

$$\boxed{b_{n-k}(\mathcal{B}_{n+1}) + b_k(\mathcal{B}_{n+1}) \geq b_k(\mathcal{C}_n) = b_{n-k}(\mathcal{C}_n)} \quad (3.8a)$$

$$\boxed{t_{n-k-1}(\mathcal{B}_{n+1}) + t_k(\mathcal{B}_{n+1}) \geq t_k(\mathcal{C}_n) = t_{n-k-1}(\mathcal{C}_n)}, \quad (3.8b)$$

⁶For example, we will allow for conical singularities, as these could be smoothed-out to a finite curvature region. Some other bordism present in the literature, such as $(\mathbb{Z}/\mathbb{Z}_2) \times \mathbb{S}_p^1$ or $(\mathbb{R} \times \mathbb{S}_p^1)/\mathbb{Z}_2$ for type IIA or IIB string theory on a periodic circle \mathbb{S}_p^1 , see [40], are not. Other bordisms in the same reference include M-theory on non-orientable manifolds. A description of these non-smooth(able) or non-orientable bordisms is out of the reach and assumptions needed to apply the algebraic topology and Morse theory tools we use, so they will not be considered.

for $k = 0, \dots, n$. As a matter of fact the first inequality is always saturated for the middle Betti numbers when n is even, in the so-called *Half lives, half dies* Theorem [104],

$$\boxed{b_{n/2}(\mathcal{B}_{n+1}) = \frac{1}{2}b_{n/2}(\mathcal{C}_n)}, \quad (3.9)$$

irrespective of the choice of bordism realization \mathcal{B}_{n+1} . In general we will expect \mathcal{B}_{n+1} to be connected and not enclosing any volume, so that $b_0(\mathcal{B}_{n+1}) = 1$ and $b_{n+1}(\mathcal{B}_{n+1}) = 0$, which further simplifies computations. Furthermore, for most of the examples considered, the torsion parts will be trivial.

Denoting $\vec{b}(\mathcal{X}_n) = (b_0(\mathcal{X}_n), \dots, b_n(\mathcal{X}_n))$, we can illustrate the above relations (3.8) and (3.9) with some examples:

- $\mathcal{C}_1 = \mathbb{S}^1$: $\vec{b}(\mathbb{S}^1) = (1, 1)$, resulting in $\vec{b}(\mathcal{B}_2) = (1, \beta, 0)$, with $\beta \geq 0$. This is precisely saturated by the disk, as $\vec{b}(\mathbb{D}^2) = (1, 0, 0)$, corresponding with Witten's BON. In general \mathbb{S}^1 can be seen as the boundary of Σ_g with a disk removed, with $\vec{b}(\Sigma_g - \mathbb{D}^2) = (1, 2g, 0)$, which for $g > 0$ can be thought of as topologically "more complicated" than \mathbb{D}^2 .
- $\mathcal{C}_2 = \Sigma_2 = \mathbb{T}^2 \# \mathbb{T}^2$: $\vec{b}(\Sigma_2) = (1, 4, 1)$, so that $\vec{b}(\mathcal{B}_3) = (1, 2, \beta, 0)$, with $\beta \geq 0$, saturated by the solid double-torus or the manifold \mathcal{B}_3 sketched in Figure 4.
- $\mathcal{C}_3 = \mathbb{T}^3$: $\vec{b}(\mathbb{T}^3) = (1, 3, 3, 1)$, so that $\vec{b}(\mathcal{B}_4) = (1, \beta_1, \beta_2, \beta_3, 0)$, with $\beta_1, \beta_2, \beta_3 \geq 0$ and $\beta_1 + \beta_2 \geq 3$. Note that (though in this case just 2) the number of possibilities saturating the inequalities is not unique. The first one of them, $\vec{b}(\mathcal{B}_4) = (1, 2, 1, 0, 0)$, corresponds with the straightforward bordism $\mathcal{B}_4 = \mathbb{T}^2 \times \mathbb{D}^2$, while $\vec{b}(\mathcal{B}_4) = (1, 1, 2, 0, 0)$ does not immediately correspond to any known 4-manifold with boundary. We will come back to this example in section 3.3 with a more involved bordism.
- $\mathcal{C}_6 = \text{K3} \times \mathbb{T}^2$: $\vec{b}(\text{K3} \times \mathbb{T}^2) = (1, 2, 23, 44, 23, 2, 1)$, resulting in $\vec{b}(\mathcal{B}_7) = (1, \beta_1, \beta_2, 22, \beta_4, \beta_5, \beta_6, 0)$, with $\beta_i \geq 0$ and $\beta_1 + \beta_5 \geq 2$ and $\beta_2 + \beta_4 \geq 23$. Note that again several possible different bordisms of X_6 (up to 72 possible solutions for $\vec{b}(\mathcal{B}_7)$) can saturate the inequalities. An evident instance of the bordism is $\vec{b}(\text{K3} \times \mathbb{S}^1 \times \mathbb{D}^2) = (1, 1, 22, 22, 1, 1, 0, 0)$.
- We finally take the lens space $\mathcal{C}_3 = L(p; q)$, with homology groups $\mathbb{Z}, \mathbb{Z}_p, 0$ and \mathbb{Z} , which unlike the previous examples has torsion. We find that $\vec{b}(\mathcal{B}_4) = (1, \beta_1, \beta_2, \beta_3, 0)$ with $\beta_i \geq 0$ for $i = 1, 2, 3$, while $t_1(\mathcal{B}_4) \geq 1$ (the rest of \mathcal{B}_4 torsion ranks can be null).

It must be emphasized that inequalities (3.8) and (3.9) are only *necessary* conditions, so a vector \vec{b} obeying them does not immediately correspond to an actual bordism.

3.2 Morse-Bott inequalities for manifolds with boundary

Once topological information for the bordism \mathcal{B}_{n+1} has been obtained, it is time to relate it with the number and type of necessary topology changes $\mathcal{C}_n \rightarrow \dots \rightarrow \emptyset$. An important tool to do this will be the ansätze (2.8) and (2.9) for the BoN solutions, such that we can split

the bordism and angular part of our solutions, and the radial direction $\rho : \mathcal{B}_{n+1} \rightarrow (-\infty, 0]$,⁷ which indicates the distance to the BoN/EotW wall. Note the following two properties of ρ :

- As given in (2.9), for $\rho \rightarrow \infty$, we can split $h_{\alpha\beta}^{\mathcal{B}}(y)dy^\alpha dy^\beta \approx d\rho^2 + h_{\bar{\alpha}\bar{\beta}}^{\mathcal{C}}dy^{\bar{\alpha}}dy^{\bar{\beta}}$, so that in this limit \mathcal{B}_{n+1} locally looks like $\mathbb{R} \times \mathcal{C}_n$. This means that in this regime $d\rho \neq 0$, as $h_{\alpha\beta}^{\mathcal{B}}$ is non-degenerate.
- As it parameterizes the smooth solution \mathcal{B}_{n+1} , we expect the critical points of ρ , i.e., where $d\rho = 0$, to be a (not necessarily connected) submanifold of \mathcal{B}_{n+1} . For technical reasons, we also ask the Hessian of ρ to be non-degenerate in the normal directions to the critical sub-manifold.⁸

The above properties mean that ρ is a *Morse-Bott function*⁹, which will allow us to use the so-called **Morse-Bott inequalities (for manifolds with boundary)** [105]. In what follows we introduce the needed mathematical machinery in order to use them.

Take for this ρ to be Morse-Bott function. Then a critical point of the boundary $p \in \text{Crit}(\rho|_{\mathcal{C}_n})$ is said to be *type N* if $\langle d\rho|_{\mathcal{C}_n}(p), n(p) \rangle < 0$, where $n(p) \in T_p\mathcal{B}_{n+1}$ is an *outward*¹⁰ normal vector to the boundary at p . We then define the following submanifolds and connected components:

$$\text{Crit}(\rho) = \{d\rho = 0\} = \bigsqcup_{j=1}^l \mathfrak{C}_j, \quad \mathcal{N}(\rho) = \{p \in \text{Crit}(\rho|_{\mathcal{C}_n}) : p \text{ is } N\} = \bigsqcup_{s=1}^{l_N} \Gamma_s. \quad (3.10)$$

We will denote by c_l and d_s the respective dimensions of \mathfrak{C}_j and Γ_s , and by λ_j and μ_s the index of ρ and $\rho|_{\mathcal{C}_n}$ over them (i.e. the number of negative eigenvalues of its Hessian at each point of the critical submanifold). These different submanifolds and concepts are depicted in Figure 4.

The *Morse-Bott counting polynomial of type N* is defined as

$$\text{MB}_t^N(\rho) = \sum_{j=1}^l P_t(\mathfrak{C}_j)t^{\lambda_j} + \sum_{s=1}^{l_N} P_t(\Gamma_s)t^{\mu_s}, \quad (3.11)$$

⁷For our purposes in this section, we will want ρ to grow towards the tip of the bordism, so we will take this definition rather than $\rho : \mathcal{B}_{n+1} \rightarrow [0, +\infty)$.

⁸If this is not the case, we can take a deformation $\rho \rightarrow \rho'$ such that the monotonous behavior of this radial direction can be captured by the $\mathcal{O}(x_\perp^2)$ terms, with x_\perp a normal direction. This is to say $\rho \sim \pm x_\perp^{2k} + \mathcal{O}(x_\perp^{2k+1}) \rightarrow \rho' \sim \pm x_\perp^2 + \mathcal{O}(x_\perp^3)$ and $\rho \sim \pm x_\perp^{2k+1} + \mathcal{O}(x_\perp^{2k+2}) \rightarrow \rho' \sim \pm x_\perp + \mathcal{O}(x_\perp^2)$.

⁹In more precise words, given \mathcal{B}_{n+1} a $(n+1)$ -dimensional compact manifold with boundary $\mathcal{C}_n = \partial\mathcal{B}_{n+1}$, a smooth function $\rho : \mathcal{B}_{n+1} \rightarrow \mathbb{R}$ is called *Morse-Bott* if the set of critical points $\text{Crit}(f) = \{p \in \mathcal{B}_{n+1} : df(p) = 0\}$ is a disjoint union of connected sub-manifolds of $\mathcal{B}_{n+1} - \mathcal{C}_n$, with each connected component being non-degenerate, and $\rho|_{\mathcal{C}_n} : \mathcal{C}_n \rightarrow \mathbb{R}$ is also Morse-Bott. Note that in principle this would also allow \mathcal{C}_n to be a manifold with boundary.

¹⁰In the sense of pointing out of the boundary \mathcal{C}_n in a direction opposite of the interior of \mathcal{B}_{n+1} , rather than an *inward* normal vector pointing towards the interior of \mathcal{B}_{n+1} . These are respectively represented by n and m in Figure 4.

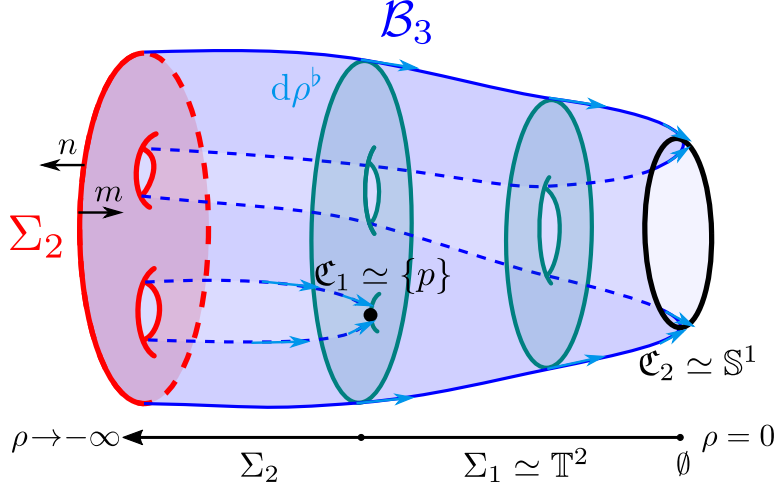


Figure 4. Sketch of the bordism \mathcal{B}_3 for the genus-2 Riemann surface Σ_2 . The different critical submanifolds of the Morse-Bott function ρ are depicted in black, $\mathfrak{C}_1 \simeq \{p\}$ ($c_1 = 0$) and $\mathfrak{C}_2 \simeq \mathbb{S}^1$ ($c_2 = 1$), both with indices $\lambda_1 = \lambda_2 = 0$. Also depicted are two *outward* and *inward* normal vectors to the boundary, n and m , as well as the vector field $d\rho^b = h^{\mathcal{B}\alpha\beta}\partial_\alpha\rho\partial_\beta = \partial^\alpha\rho\partial_\alpha$ associated to ρ , in blue. Depicted in green are the internal 2-manifold at two fixed values of ρ .

where $P_t(\mathcal{M}) = \sum_{j=0}^{\dim \mathcal{M}} b_j(\mathcal{M})t^j$ is the Poincaré polynomial of a given manifold \mathcal{M} . Then the *Morse-Bott inequalities for manifolds with boundary* state that for \mathcal{B}_{n+1} a compact manifold with boundary and ρ a Morse-Bott function defined over it, there exists a polynomial $R \in \mathbb{Z}_{\geq 0}[t]$ with non-negative integer coefficients such that

$$\boxed{\text{MB}_t^N(\rho) - P_t(\mathcal{B}_{n+1}) = (1+t)R(t)} \quad (3.12)$$

From the behavior of ρ , as it is constant in \mathcal{C}_n for $\rho \rightarrow \infty$, which we identify with the boundary of \mathcal{B}_{n+1} , $\mathcal{N}(\rho) = \mathcal{C}_n$, with $\mu = 0$, so that

$$\boxed{\sum_{j=1}^l P_t(\mathfrak{C}_j)t^{\lambda_j} + P_t(\mathcal{C}_n) - P_t(\mathcal{B}_{n+1}) = (1+t)R(t)} \quad (3.13)$$

for some $R(t) \in \mathbb{Z}_{\geq 0}[t]$. Note that evaluating at $t = -1$, we have $\chi(\mathcal{B}_{n+1}) = \chi(\mathcal{C}_n) + \sum_{j=1}^l (-1)^{\lambda_j} \chi(\mathfrak{C}_j)$, with $\chi(\mathcal{M})$ the Euler characteristic of \mathcal{M} .

Topology changes occur when internal cycles shrink over critical submanifolds \mathfrak{C} of ρ , with $d\rho = 0$ indicating that such cycle no longer “propagates” as we move towards the BoN/EotW brane. The dimensionality of the “disappearing” cycle is given by $c + \lambda - 1$, where $c = \dim \mathfrak{C}$ and λ its critical index, as $\lambda - 1$ dimensions shrink (one has to discount the radial direction) over the c -dimensional base the cycle is fibered over. Furthermore, apart from this $(c + \lambda - 1)$ -cycle \mathcal{A} that shrinks (what we could interpret as a cobordism for \mathcal{A} into nothing), the dual $(n - c - \lambda + 1)$ -cycle \mathcal{A}' also disappears, not shrinking *per se* but being interpreted now as a chain

with boundary at \mathcal{C} . This results in a reduction of the homology groups $H_{c+\lambda-1}(\rho^{-1}(r); \mathbb{Z})$ and $H_{n-c-\lambda+1}(\rho^{-1}(r); \mathbb{Z})$ for r smaller and larger than r_* , with r_* the location of the critical point, which translates into a lowering (not necessarily by a unit) of the respective Betti numbers and/or torsion ranks. We will revisit this cycle shrinking/transforming into a chain with boundary interpretation when discussing flux potentials and their fate after topology changes in section 4.2.

Analogously, it could be the case that the topology change results in the creation of some cycle (and its dual), as occurs in Figure 3b or by the nucleation of a baby Universe that might reattach later or not, but both of these cases the cobordism into nothing will feature more topology changes than necessary.

The number l of critical submanifolds will corresponds to the number of topology changes (including the ultimate collapse into nothing), so impossibility to satisfy (3.13) with $l = 1$ means an intermediate topology change must occur. Note that the index of the critical submanifold is given by $\lambda+c-1 = n$, as all dimensions must close at the top of the BoN/EotW brane.

Inequalities 3.13 only consider the free part of the homology groups (i.e. the Betti numbers), with the torsion ranks not entering into account. While most of the examples considered will not feature torsion, one would expect that bordisms with torsion will probably require additional topology changes in order to get rid of this topological charge. Unfortunately, to our knowledge there are not results concerning Morse-Bott inequalities for manifolds with boundary *and torsion* in the Mathematics literature. The closest result are the *Morse-Pitcher inequalities* [106] for closed manifolds without boundary (but with torsion). Having $\rho : \mathcal{M}_n \rightarrow \mathbb{R}$ a *Morse* function (this is, critical loci will be isolated points rather than general submanifolds, as in Morse-Bott functions), then

$$m_\lambda \geq b_\lambda(\mathcal{M}_n) + t_\lambda(\mathcal{M}_n) + t_{\lambda-1}(\mathcal{M}_n) \quad (3.14a)$$

$$\sum_{k=0}^{\lambda} (-1)^{\lambda-k} m_k \geq \sum_{k=0}^{\lambda} (-1)^{\lambda-k} b_k(\mathcal{M}_n) + t_\lambda(\mathcal{M}_n), \quad (3.14b)$$

for $\lambda = 1, \dots, n$, where m_λ is the number of critical points of ρ with index λ . While it is clear that having torsion on \mathcal{B}_{n+1} will probably result in more critical points (and topology changes) appearing, it is not clear the way this can be quantified. In section 5.1 we will apply the above (3.14) to study collision of bubbles of nothing.

Topology changes associated to an internal cycle shrinking into a point and disappearing are associated, from the EotW brane point of view, with the moduli that controlled its size in the original EFT blowing up to infinity. If the rest of cycles and the whole manifold remain relatively unaltered, which can be considered to be a good approximation in the large volume regime, then the critical exponent δ from (2.16) could be read from the dependence of said blowing up scalar in the potential. If the different topology changes are spaced in the ρ spatial direction, then a EFT description is valid between the different domain walls, and critical

exponents can be associated with distinct topology changes/types of critical points, though not necessarily in a 1-to-1 basis. An example of these are flux potentials from p -form fluxes threading different internal cycles, as we will see in section 4 in different examples.

3.2.1 Some easy examples

We will now consider some ubiquitous compactification manifolds to test and illustrate this.

Example 1: Spheres \mathbb{S}^n Our first example is the n -dimensional sphere, which is known to be the boundary of the solid ball \mathbb{D}^{n+1} . One way one can imagine the compactification to interpolate to nothing is by shrinking the radial direction to a single point, so that $\text{Crit}(\rho) = \{p\}$ with index $\lambda = n + 1$. As $P_t(\mathbb{S}^n) = 1 + t^n$ and $P_t(\mathbb{D}^{n+1}) = 1$, one has that (3.13) translates to

$$(1+t)R(t) = 1 \times t^{n+1} + (1+t^n) - 1 = (1+t)t^n \implies R(t) = t^n \in \mathbb{Z}_{\geq 0}[t], \quad (3.15)$$

so indeed the Morse-Bott inequalities are satisfied with a single topology change.

Example 2: Tori \mathbb{T}^n Due to their simplicity and control, some of the most studied compactifications in the literature are toroidal manifolds. Surprising nobody, they can also be taken to nothing without intermediate topology changes. Indeed, as $\mathbb{T}^n = \mathbb{T}^{n-1} \times \mathbb{S}^1$, one can interpolate to nothing by shrinking one of the 1-cycles over the \mathbb{T}^{n-1} base. This way, using $P_t(\mathbb{T}^n) = (1+t)^n$

$$(1+t)R(t) = (1+t)^{n-1}t^2 + (1+t)^n - (1+t)^{n-1} \cdot 1 = (1+t)^n(t-1) = t(1+t)^n, \quad (3.16)$$

so that one can take $R(t) = t(1+t)^{n-1}$, which means that on principle intermediate topology changes are not necessary for BoN with compact manifold \mathbb{T}^n . We will see in section 4.3 more involved bordisms of toroidal compactifications which include additional topology changes.

Example 3: Product manifolds An immediate corollary follows for product manifolds $\mathcal{C}_n = \mathcal{X}_m \times \mathcal{Y}_{n-m}$ (both manifolds without boundary) in which \mathcal{X}_m can go to nothing without intermediate topology changes. In other words, there exists a $(m+1)$ -smooth manifold \mathcal{D}_{m+1} with $\partial\mathcal{D}_{m+1} = \mathcal{X}_m$, a Morse-Bott function $\rho : \mathcal{D}_{m+1} \rightarrow [0, +\infty)$ with a single critical submanifold $\mathfrak{C} \subset \mathcal{D}_{m+1}$ and polynomial $R(t) \in \mathbb{Z}_{\geq 0}[t]$ such that

$$P_t(\mathfrak{C})t^{m-\dim\mathfrak{C}} + P_t(\mathcal{Y}_m) - P_t(\mathcal{D}_{m+1}) = (1+t)R(t). \quad (3.17)$$

Now, defining $\mathcal{B}_{n+1} = \mathcal{D}_{m+1} \times \mathcal{Y}_{n-m}$, we have $\partial\mathcal{B}_{n+1} = (\partial\mathcal{D}_{m+1} \times \mathcal{Y}_{n-m}) \cup (\mathcal{D}_{m+1} \times \partial\mathcal{Y}_{n-m}) = \mathcal{X}_m \times \mathcal{Y}_{n-m} = \mathcal{C}_n$, thus providing a bordism realization for X_n . We can then extend the Morse-Bott function

$$\hat{\rho} : \mathcal{B}_{n+1} = \mathcal{D}_{m+1} \times \mathcal{Y}_{n-m} \longrightarrow [0, +\infty), \quad (3.18)$$

$$(y, z) \longmapsto \rho(y),$$

such that the only critical submanifold of $\hat{\rho}$ is $\hat{\mathcal{C}} = \mathcal{C} \times Z_{n-m}$. Finally, using $P_t(A \times B) = P_t(A)P_t(B)$, we obtain

$$P_t(\hat{\mathcal{C}})t^{m-\dim \mathcal{C}} + P_t(\mathcal{C}_n) - P_t(\mathcal{B}_{n+1}) = (1+t)R(t)P_t(\mathcal{Y}_{n-m}) . \quad (3.19)$$

As the Poincaré polynomial always has non-negative coefficients, $R(t)P_t(\mathcal{Y}_{n-m}) \in \mathbb{Z}_{\geq 0}[t]$, so that on principle there is no need for intermediate topology changes in $\mathcal{C}_n = \mathcal{X}_M \times \mathcal{Y}_{n-m}$ going to nothing. As we will see in section 4.4, this does not extend to non-trivial fibrations.

3.3 Non-minimal bordisms and defects

In the above sections only the global topology (actually only the homology groups) of the bordism \mathcal{B}_{n+1} was considered, assuming from the start that the relevant bordism groups $\Omega_n^{\mathfrak{g}}$ vanished. However, as explained in section 1, in order for this to happen there might be extra ingredients or *defects* that must be added to our theory, such that $\Omega_n^{\mathfrak{g}} \neq 0 \rightarrow \Omega_n^{\mathfrak{g}+\text{def.}} = 0$. In a general way, $\Omega_k^{\mathfrak{g}} \neq 0$ implies the existence of a $D - k - 1$ -global symmetry in our theory, with associated conserved topological charge/invariant [40]

$$Q : \begin{array}{l} \Omega_k^{\mathfrak{g}} \longrightarrow \mathbb{Z} \\ [\mathcal{M}_k] \longmapsto \int_{\mathcal{M}_k} G_k \end{array} , \quad (3.20)$$

where G_k is some associated closed k -form. Note that by definition Q is independent of the bordism representative. Now, in order to kill this bordism invariant, a $D - k - 1$ defect is needed. For the case of oriented bordisms in the presence of A_p forms, $\Omega_{p+1}^{SO, A_p} \simeq \mathbb{Z}$, represented by the magnetic charge Q above. The $D - (p + 1) - 1 = D - p - 2$ defects are given by the $D(D - p - 3)$ -branes on whose world-volume the magnetic dual gauge potential \tilde{A}_{D-p-2} lives (see [40] for more details on this).

In general, when compactifying on \mathcal{C}_n to $d = D - n$ dimensions, we will also have internal k -cycles over which topological charges can be defined. The $d + n - k - 1$ -defects associated with $\{\Omega_k^{\mathfrak{g}}\}_{k=0}^n$ will allow the associated k -cycles to go to nothing in the intermediate topology changes described in section 3.2. As at the different sides of the topology change (3.1) the compactification manifold $\mathcal{C}_n^{(k)} \rightarrow \mathcal{C}_n^{(k+1)}$ will be different, the lower d -dimensional EFT will change, with the $d + n - k - 1$ -defects being seen from the macroscopic point of view as codimension-1 $d - 1$ -domain walls, which are localized at the topology change loci. Depending on how the additional $n - k$ directions are wrapped, we can have the following two types of domain walls:

- **Thin domain walls:** The $d + n - k - 1$ -defect extends over $d - 1$ of the macroscopic directions, while wrapping the $n - k$ -cycle dual to the k -cycle in \mathcal{C}_n supporting the topological charge, and that the defect allows to shrink to nothing. Note that after the topology change the dual $n - k$ -cycle no longer exists either, so the domain wall also acts as a boundary of both cycles. An illustration of this is depicted in Figure 5a, and will found in explicit examples in section 4.2.

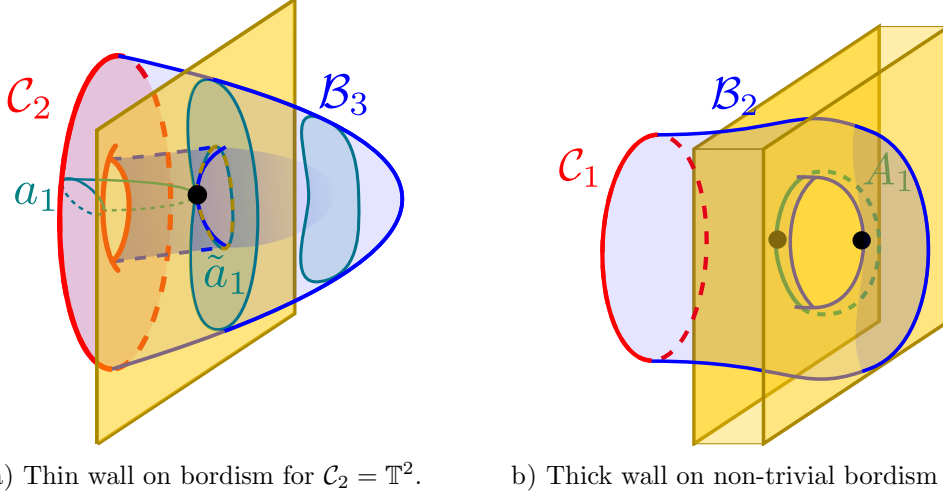


Figure 5. Illustrations of thin and thick walls in different bordisms, respectively for $C_2 = \mathbb{T}^2$ (subfigure 5a) and $C_1 = \mathbb{S}^1$ (subfigure 5b). In the thin wall case the $(d+n-k-1 = d)$ -defect simply extends over $d-1$ spacetime directions and wrapping along the $(n-k=2-1=1)$ -cycle \tilde{a}_1 dual to the 1-cycle a_1 that is shrinking. In the thick wall case the analogous d -defect extends over $d-1$ spacetime directions and wraps a 1-cycle A_1 of $\mathcal{B}_2 \simeq \mathbb{T}^2 - \mathbb{D}^2$. This second example can be found in section 7.3 from [107].

- **Thick domain walls:** The $d+n-k-1$ -defect extends over $d-1$ macroscopic directions (perpendicular to the bordism radial direction ρ), while wrapping a $n-k$ -cycle in the bordism \mathcal{B}_{n+1} , in such a way that the cycle also extends in the ρ direction (for a finite interval), with the $n-k$ -cycle not corresponding to any specific cycle in any of the $\mathcal{C}_n^{(k)}$ slices. Note that in this case the localization occurs around said cycle, which by definition is non-contractible, unlike those of $\mathcal{C}_n^{(k)}$ once embedded in \mathcal{B}_{n+1} .

This is illustrated in Figure 5b, with an example for this disposition being found in section 7.3 of [107] (albeit not in the context of an explicit BoN construction), the non-trivial 1-cycle $A_1 \subset \mathcal{B}_2$ has a monodromy that kills the \mathbb{Z}_3 factor of $\Omega_1^{\text{Spin-Mp}(2,\mathbb{Z})} \simeq \mathbb{Z}_8 \oplus \mathbb{Z}_3$ by performing a reflection $g \rightarrow g^{-1}$ on the generator of $\mathbb{Z}_3 = \langle g \rangle$ (we refer to the original, [107] for more details). This is equivalent to having a 8-defect spanning between the two critical points (in black in Figure 5b) associated to A_1 , resulting in a *thick* (7+1)-domain wall.¹¹

The defects considered here in general are of stringy origin and will backreact on the spacetime geometry, resulting in a loss of the smooth geometry (e.g. conical defects and angular deficits). We expect that, in some of these cases, the topological description of our bordism to hold in a way that can be smoothed-out and the Morse-Bott inequalities hold.

With respect to thick domain walls, in order for the defects or non-trivial geometry (such as monodromies in the above example) to wrap internal (non-contractible) cycles of

¹¹We thank Markus Dierigl and Miguel Montero for referencing a specific example of this class to us.

the bordism, it will be required that the topology of \mathcal{B}_{n+1} is more involved than the minimal structure required from 3.8. As we will see in section 4.3, this can also be the case in order to include the necessary (in this case Spin) defects while holding a smooth description of the bordism.

4 Some more physical examples

After the theoretical introduction and mathematical results from the previous sections, we will now consider some relatively realistic constructions, as well as the qualitative properties of the cobordisms to nothing/end of the world branes.

4.1 Spheres with fluxes

We first begin by considering a pretty straightforward examples. Take for this the 10d Einstein-dilaton-RR sector of the type II bosonic supergravity action in Einstein frame [108, 109],

$$S_{\text{II}} \supseteq \int d^{10}x \sqrt{-G_{10}} \left\{ \mathcal{R}_{10} - (\partial\hat{\Phi})^2 - \frac{1}{2n!} e^{\frac{5-n}{\sqrt{2}}\hat{\Phi}} |F_n|^2 \right\}, \quad (4.1)$$

where $\hat{\Phi}$ is the canonically normalized 10 dimensional dilaton, and for simplicity we have considered a single RR field strength. One can compactify the above theory on a n -sphere \mathbb{S}^n with volume \mathcal{V} in $M_{\text{Pl},10}$ units and N units of flux, which assuming that F_p only has internal legs, results in a scalar potential in the $(d = 10 - n)$ -dimensional EFT from the curvature and flux contributions:

$$\kappa_d^2 V(\hat{\Phi}, \rho) = -\frac{\pi}{2} (10-d)(9-d) \Gamma\left(6 - \frac{d}{2}\right)^{-\frac{2}{10-d}} e^{-2\sqrt{\frac{8}{(10-d)(d-2)}}\rho} + \frac{N^2}{4} e^{\frac{d-5}{\sqrt{2}}\hat{\Phi} - (d-1)\sqrt{\frac{10-d}{2(d-2)}}\rho}, \quad (4.2)$$

where $\rho = \sqrt{\frac{8}{(10-d)(d-2)}} \log \frac{\mathcal{V}}{\mathcal{V}_0}$ is the canonically normalized radion, with $\mathcal{V}_0 = \left(\frac{\kappa_{10}}{\kappa_d}\right)^2$ some fixed volume. While for $d = 5$ (precisely when $\hat{\Phi}$ is not sourced by the RR field strength, see (4.1)) (4.2) only depends on the volume $\mathcal{V} \sim N^{\frac{5}{4}}$ and has an AdS minimum $V_{\text{AdS}} \sim -N^{-\frac{4}{3}}$ which becomes deeper as N decreases, for $d \neq 5$ the potential gradient flow pushes towards large volume configurations and small/large coupling (depending on the sign of $5 - d$), with $\hat{\Phi} = \sqrt{\frac{d-2}{10-d} \frac{d-9}{5-d}} \rho$.

Now, as explained in section 3.3, the inclusion of $(p-1)$ -forms in our theory (which act as gauge potentials for the RR field strength) results in a conserved topological charge (the flux number) upon compactification on oriented surfaces such as \mathbb{S}^p . In order to kill the $\Omega_p^{SO, A_{p-1}}$ invariant, $D(8-p)$ -brane defects must be included. Precisely this $D(8-p)$ -brane will act as the EotW brane, with the \mathbb{S}^p sphere shrinking as we approach it. This was studied in more generality in [78], to which we refer for more detail. In general the inclusion of a D-brane results in a singular term in the EFT action, and as such the bordism \mathcal{B}_{p+1} will have a conical singularity at its tip, where the D_p -brane is located. However, we still have $\mathcal{B}_{p+1} \simeq \mathbb{D}^{p+1}$,

and so we can still consider a smooth structure on the bordism and the results from section 3.

In the presence of F_n RR flux, a $D(8-n)$ brane (with $n = 2, \dots, 7$)¹² solution to (4.1) has the following 10d Einstein metric and $\hat{\Phi}$ profiles [108]:

$$ds_{10}^2 = Z(r)^{\frac{1-n}{8}} \underbrace{\eta_{\mu\nu} dx^\mu dx^\nu}_{dx_{\parallel}^2} + Z(r)^{\frac{7-n}{8}} \underbrace{(dr^2 + r^2 d\Omega_{8-n}^2)}_{dx_{\perp}^2} \quad (4.3a)$$

$$\hat{\Phi} = \frac{n-5}{4\sqrt{2}} \log Z(r) + \hat{\Phi}_{\infty}, \quad \text{where} \quad Z(r) = 1 + \left(\frac{r_0}{r}\right)^{n-1}, \quad (4.3b)$$

where r is a radial direction perpendicular to the brane and r_0 is a length scale given by

$$r_0 = \sqrt{\alpha'} \left[(4\pi)^{\frac{n-3}{2}} \Gamma\left(\frac{n-1}{2}\right) e^{\sqrt{2}\hat{\Phi}_{\infty}} N \right]^{\frac{1}{n-1}}, \quad (4.4)$$

explicitly depending on the flux number N . For $n = 5$ (i.e. D3 branes), the dilaton does not blow up at $r = 0$ (and as commented above results in an AdS minimum with a flat direction for $\hat{\Phi}$ upon compactification), and the D3 brane will not correspond with the EotW brane description from section 2.2, as there is neither a cycle shrinking or a scalar going to infinity.¹³ We will thus not consider this case and remain with $n \neq 5$.

Upon compactification on \mathbb{S}^n (transversal to the brane) down to $d = 10 - n$ dimensions, the $D(8-n = d-2)$ -brane has now spatial codimension one (as expected from EotW branes), with the Einstein frame metric and the radion profile now given by [78]

$$ds_d^2 = \left[\left(\frac{r}{r_0}\right)^2 Z(r)^{\frac{d-1}{8}} \right]^{\frac{10-d}{d-2}} \left\{ Z(r)^{\frac{d-9}{8}} \eta_{\mu\nu}^{\perp} dx^\mu dx^\nu + Z(r)^{\frac{d-1}{8}} dr^2 \right\} \quad (4.5a)$$

$$\rho(r) = \sqrt{\frac{2(10-d)}{d-2}} \log \left[\left(\frac{r}{r_0}\right)^2 Z(r)^{\frac{d-1}{8}} \right], \quad (4.5b)$$

where now the volume scales as

$$\frac{\mathcal{V}(r)}{\mathcal{V}_0} = e^{\frac{1}{2}\sqrt{\frac{(d-2)(10-d)}{2}}\rho(r)} = \left(\frac{r}{r_0}\right)^{10-d} Z(r)^{\frac{(10-d)(d-1)}{2}}, \quad (4.6)$$

¹²We do not consider D8- and D7-branes as their backreaction prevents asymptotically flat spacetime, complicating the analysis.

¹³In this $d = 5$ the cobordism to nothing is more subtle [24], occurring through nucleation of D3-branes that eat up units of flux charge, $N \rightarrow N - 1$, in such a way that the minimum of the potential $V_{\text{AdS}} \sim -N^{-4/3}$ becomes deeper and the \mathbb{S}^5 shrinks, $\mathcal{V} \sim N^{5/4}$. In the $N \rightarrow 0$ limit the AdS curvature radius goes to zero and the 5-sphere shrinks to a point. Though this does not happen in a remotely smooth way either (the integer flux jumps when crossing each brane), from the topological point of view the cobordism to nothing still corresponds in the sphere shrinking to a point without intermediate topology changes. See also [18], where a (non-smooth) BoN solution for the non-supersymmetric $\text{AdS}_5 \times \mathbb{S}^5/\mathbb{Z}_k$ is built, based in the Hopf fibration structure $\mathbb{S}^1 \hookrightarrow \mathbb{S}^5/\mathbb{Z}_k \rightarrow \mathbb{C}\mathbb{P}^2$, with the \mathbb{S}^1 fiber shrinking over the $\text{AdS}_5 \times \mathbb{C}\mathbb{P}^2$ similarly to Witten's BoN.

with $V(r) \rightarrow 0$ as $r \rightarrow 0$ except for $d = 5$ (equivalently $n = 5$ or D3 branes), where the volume remains finite, and indeed the $D(d-2)$ -branes serve as EotW branes, coinciding with the tip of the \mathbb{S}^{10-d} bordism to nothing, topologically given by the solid disk \mathbb{D}^{11-d} . The $\Omega_{d-2}^{SO, A_{10-d}}$ defect given by the D-brane is precisely located in the topology change (in this case into nothing).

For completion, we refer to [78], where these solutions were studied with the EotW brane formalism, with the following critical exponent¹⁴

$$\delta = \frac{2|d-5|}{\sqrt{(d-2)(11-d)}} = \frac{2|5-n|}{\sqrt{(8-n)(n+1)}} \quad (4.7)$$

was computed, with again $\delta = 0$ for $d = n = 5$. Note that for these examples there is a 1-to-1 correspondence between the dimensionality of the sphere shrinking to a point and the critical exponent.

The above description only discusses the local EotW behavior of the scalars as they approach the brane/cobordism wall and the sphere threaded by fluxes shrinks to a point, which as we have argued for and seen can happen without intermediate topology changes. Actual vacuum instability solutions corresponding to BoN are much more involved, and we will not detail them. For this we refer to the literature, such as [19–22, 27, 73, 75].

4.2 Type IIB string theory on compact Riemann surfaces

We will now consider a more involved example with actual intermediate topology changes being needed in order to have a smooth(able) bordism to nothing, and study how this intermediate changes in the internal dimension affect the lower-dimensional EFT. The most straightforward construction for this is Type IIB string theory compactified on a Riemann surface Σ_g of genus $g \geq 2$.

For simplicity, we will not consider the full $\text{Spin} - GL^+(2, \mathbb{Z})$ bordism of type IIB string theory¹⁵ and simply restrict to Spin bordism, with [40, 67]

$$\Omega_1^{\text{Spin}} = \langle \mathbb{S}_p^1 \rangle \simeq \mathbb{Z}_2, \quad \Omega_2^{\text{Spin}} = \langle \mathbb{S}_p^1 \times \mathbb{S}_p^1 \rangle \simeq \mathbb{Z}_2. \quad (4.9)$$

If we further take Σ_g to be oriented and include the p -fields in the 10d SUGRA description,

¹⁴This critical exponent can also be immediately computed by obtaining the exponential rate of potential (4.2) along the trajectory $\hat{\Phi} = \sqrt{\frac{d-2}{10-d} \frac{d-9}{5-d}} \rho$ the scalars follow for $d \neq 5$.

¹⁵Type IIB string theory has fermions and a duality group $SL(2, \mathbb{Z})$, which after including the F-theory torus reflections (and their action on fermions) is promoted to $GL^+(2, \mathbb{Z})$ [110, 111]. This way, the actual structure our bordism must take into consideration is $\text{Spin} - GL^+(2, \mathbb{Z})$ (see [52, 107, 112] for more on this, including the rest of cobordism groups and generators, as well as properties of the required defects), with

$$\Omega_1^{\text{Spin} - GL^+(2, \mathbb{Z})} = \langle \{\mathbb{S}_R^1, L_4^1\} \rangle \simeq \mathbb{Z}_2 \oplus \mathbb{Z}_2, \quad \Omega_2^{\text{Spin} - GL^+(2, \mathbb{Z})} = \langle \mathbb{S}_p^1 \times \mathbb{S}_R^1 \rangle \simeq \mathbb{Z}_2, \quad (4.8)$$

where \mathbb{S}_p^1 is the circle with periodic boundary conditions, \mathbb{S}_R^1 is the circle with a non-trivial $GL^+(2, \mathbb{Z})$ reflection bundle, and $L_4^1 \simeq \mathbb{S}^1/\mathbb{Z}_4$ a Lens space, naturally endowed with a \mathbb{Z}_4 bundle.

as explained in section 3.3, D-branes will have to be include in order to “eat” the magnetic charges of the fluxes.

Before studying the 8d EFT description after compactifying on the Riemann surface, let’s study how many and how the topology changes occur.

Morse-Bott inequalities for Σ_g

For our purposes, a Riemann surface Σ_g is determined by its genus g and its Spin structure. Having no torsion, homology is set by the Betti numbers $\vec{b}(\Sigma_g) = (1, 2g, 1)$, so there are $b_1(\Sigma_g) = 2g$ 1-cycles, paired in intersecting dual cycles. By using (3.8) and (3.9), the Poincaré polynomial of the bordism \mathcal{B}_3 is $P_t(\mathcal{B}_3) = 1 + gt$.¹⁶ Because of the low dimensionality we are working with, the only possible critical submanifolds are $\{p\}$ and \mathbb{S}^1 , of dimension $c = 0$ and $c = 1$, respectively. Now, as at each critical locus with index λ we have a $(\lambda + c - 1)$ -cycle shrinking to nothing, this only allows us to have **(a)** a 1-cycle collapsing on a point, **(b)** a 1-cycle collapsing on \mathbb{S}^1 , or **(c)** a 2-cycle without internal cycles¹⁷ collapsing on a point. As the two last possibilities saturate the $\lambda + c - 1 \leq 2 = \dim \Sigma_g$ inequality, and thus correspond to the final topology change into nothing, there can only be one of them.

Considering (a, b, c) topology changes of the above types (i.e., a total $N = a + b + c$ topology changes), the Morse-Bott inequalities will be given by

$$at^2 + b(1+t)t^2 + ct^3 + (1+2gt+t^2) - (1+gt) = (1+t)R(t), \quad (4.10)$$

with $R(t) \in \mathbb{Z}_{\geq 0}[t]$ and $b+c=1$. In order to have $1+t$ being a factor of the LHS of the above equation, it is needed that $a = g + c - 1$. This results in the following options, depending on the genus g :

- $g = 0$: The sphere $\Sigma_0 = \mathbb{S}^2$ shrinks to nothing in a single topology change, with $(a, b, c) = (0, 0, 1)$.
- $g = 1$: For the torus $\Sigma_1 = \mathbb{T}^2$ it is possible to go to nothing via one of the 1-cycles shrinking over its dual, so $(a, b, c) = (0, 1, 0)$. It is also possible to have two topology changes, with a 1-cycle pinching over a point, leading to a sphere that later shrinks, $\mathbb{T}^2 \rightarrow \mathbb{S}^2 \rightarrow \emptyset$, $(a, b, c) = (1, 0, 1)$.
- $g \geq 2$: The contribution of $a = g + c - 1$ to the total number of topology changes is minimized by $(a, b, c) = (g - 1, 1, 0)$. As each **(a)**-type topology change “kills” a pair of dual 1-cycles, this results in a final $\Sigma_1 = \mathbb{T}^2$ which shrinks through a type-**(b)** topology change, with a total $N = g$. An extra **(a)** and **(c)** can be in place of the last **(b)**, amounting for $N = g + 1$.

This way, a bordism (that does not increment the number of internal components or 1-cycles) between Σ_g and nothing features either g ($g - 1$ type **(a)** and a final **(b)**) or $g + 1$

¹⁶Riemann surfaces automatically set the Betti numbers of their bordism to nothing (assuming it has a single connected component), as the *Half dies, half lives* theorem implies $b_1(\mathcal{B}_3) = \frac{1}{2}b_1(\Sigma_g) = g$.

¹⁷If torsion has not been induced on \mathcal{B}_3 , this is then \mathbb{S}^2 shrinking.

(*g* type **(a)** and a final **(c)**) topology changes. At each of these the compact manifold will change as we move in the ρ direction of the bordism, resulting in different low-energy EFTs behind each domain wall.

In Appendix A some basics about Riemann surfaces and their shape moduli are presented. While the final shrinking of \mathbb{T}^2 or \mathbb{S}^2 (type **(b)** or **(c)** topology changes from the above description) is well understood, accounting simply for a compactification limit in the EotW brane description, type **(a)** changes, with a 1-cycle pinching on a point and decaying, is not as simple. This can be well understood through tachyon condensation from a world-sheet perspective [113, 114]. In Appendix B we give a brief overview of how 1-cycles of Riemann surfaces with anti-periodic boundary conditions decay once their thickness at some point of the handle becomes small enough, with tachyon condensation effectively preventing spacetime degrees of freedom from propagating along the handle direction.

The low-energy EFT(s) under topology changes

After the needed introductory remarks, we can proceed to study the changes in the lower-dimensional EFT under the topology changes. To do so, we first take the 10D Type IIB SUGRA bosonic effective action in Einstein frame [108, 109]

$$S_{\text{IIB}} \supseteq \frac{1}{2\kappa_{10}^2} \left\{ \int d^{10}x \sqrt{-G} \left[\mathcal{R}_G - \frac{1}{2}(\partial\Phi)^2 - \frac{e^{-\Phi}}{2}|H_3|^2 - \frac{e^\Phi}{2}|F_1|^2 - \frac{e^{\frac{\Phi}{2}}}{2}|\tilde{F}_3|^2 - \frac{1}{2}|\tilde{F}_5|^2 \right] - \frac{1}{2} \int C_4 \wedge H_3 \wedge dC_2 \right\}, \quad (4.11)$$

where $|\omega_p|^2 = \omega_p \wedge \star \omega_p$, Φ is the 10-dimensional dilaton and

$$H_3 = dB_2, \quad F_1 = dC_0, \quad \tilde{F}_3 = dC_2 - C_0 H_3, \quad \tilde{F}_5 = dC_4 - \frac{1}{2}C_2 \wedge dB_2 + \frac{1}{2}B_2 \wedge dC_2. \quad (4.12)$$

For simplicity, we will set $C_2, C_4 \equiv 0$, under which (4.11) simplifies to

$$S'_{\text{IIB}} \supseteq \frac{1}{2\kappa_{10}^2} \int d^{10}x \sqrt{-G} \left\{ \mathcal{R}_G - \frac{1}{2}(\partial\Phi)^2 - \frac{e^{-\Phi} + C_0^2 e^{\frac{\Phi}{2}}}{2}|H_3|^2 - \frac{e^\Phi}{2}|F_1|^2 \right\}, \quad (4.13)$$

again considering only the bosonic part. We now compactify our theory on a Riemann surface Σ_g , with volume \mathcal{V} in 10d Planck units. Taking the legs of F_1 and one of H_3 lay on Σ_g , the following 8d effective action results:

$$S_{\Sigma_g} = \frac{1}{2\kappa_8^2} \int \left\{ \star [\mathcal{R} - 2V(\vec{\varphi})] - G_{ab}(\vec{\varphi}) d\varphi^a \wedge \star d\varphi^b - \frac{1}{2} \mathcal{A}_{AB}(\vec{\varphi}) H_2^A \wedge \star H_2^B \right\}, \quad (4.14)$$

where here $\vec{\varphi} = (\Phi, \mathcal{V}, \vec{\tau})$ are the moduli corresponding to the 10d dilaton, Σ_g volume and complex structure (respectively 0, 1 and $3(g-1)$ for $g = 0, 1$ or more), and

$$H_2^A \equiv dB_1^A = \int_{a_A} H_3, \quad A = 1, \dots, 2g \quad (4.15)$$

are the field strengths of some effective 1-forms obtained from integrating H_3 along the $2g$ 1-cycles of Σ_g , with gauge kinetic matrix

$$\mathcal{A}_{AB}(\vec{\varphi}) = \left(\frac{\mathcal{V}}{\mathcal{V}_0} \right)^{\frac{1}{3}} (e^{-\Phi} + C_0^2 e^{\frac{\Phi}{2}}) \mathbb{A}_{AB}(\vec{\tau}), \quad (4.16)$$

where $\mathbb{A}_{AB}(\vec{\tau})$ is a positive definite symmetric matrix with $\det \mathbb{A} = 1$, given in terms of the period matrix Ω , depending only on the complex structure moduli $\vec{\chi}$. It is given, as derived in Appendix A, by (A.18), [113, 114]

$$\mathbb{A} = i \begin{pmatrix} 2\Omega(\Omega - \bar{\Omega})^{-1}\bar{\Omega} & -(\Omega + \bar{\Omega})(\Omega - \bar{\Omega})^{-1} \\ -(\Omega + \bar{\Omega})(\Omega - \bar{\Omega})^{-1} & 2(\Omega - \bar{\Omega})^{-1} \end{pmatrix}, \quad (4.17)$$

which for $g = 1$ simplify to the following 2×2 real matrix

$$\mathbb{A} = \tau_2^{-1} \begin{pmatrix} \tau_1^2 + \tau_2^2 & -\tau_1 \\ -\tau_1 & 1 \end{pmatrix}. \quad (4.18)$$

Regarding the scalar potential, it has contributions both from the Σ_g internal curvature and the different fluxes, with

$$\begin{aligned} V(\varphi) &= -\frac{1}{2} \left(\frac{\mathcal{V}}{\mathcal{V}_0} \right)^{-\frac{4}{3}} \int_{\Sigma_g} d^2y \sqrt{g_{\Sigma}} \mathcal{R}_{\Sigma} + \frac{1}{2} \left(\frac{\mathcal{V}}{\mathcal{V}_0} \right)^{-\frac{4}{3}} e^{\Phi} \int_{\Sigma_g} F_1 \wedge \star F_1 \\ &= \left(\frac{\mathcal{V}}{\mathcal{V}_0} \right)^{-\frac{4}{3}} \left[\pi(g-1) + \frac{1}{2} e^{\Phi} \sum_{I=1}^{2g} Q^{I\top} \mathbb{A}(\vec{\chi}) Q^I \right], \end{aligned} \quad (4.19)$$

where Gauss-Bonnet theorem has been used, and $Q^{Ii} = \int_{a_i} F_I$ are the charges vectors of the different F_1 components with respect to the homology basis. It is easy to see that for $g \geq 1$ $V(\varphi) \geq 0$ and negative for $g = 0$ (note that for $g = 0$ there is no flux potential), with gradient flows respectively pointing to $\mathcal{V} \rightarrow \infty$, $\Phi \rightarrow 0$ and $\mathcal{V} \rightarrow 0$.

As for the complex structure moduli, these are stabilized for a generic flux configuration of F_1 [113].¹⁸ Note that, as explained in Appendix B, for the topology change to occur it

¹⁸To see this, notice that all the eigenvalues $\mathcal{A}_{AB} \propto \mathbb{A}_{AB}$ are positive. From the definition (A.7) of the period matrix Ω^{ij} , in a topology change $\Sigma_g \rightarrow \Sigma_{g-1}$ a 1-cycle pinches and becomes small, and as such some eigenvalue of $\text{Im}\Omega = \frac{1}{2i}(\Omega - \bar{\Omega})$ goes to 0, or equivalently, one of $(\Omega - \bar{\Omega})^{-1}$ blows up. Then in such a limit $\mathbb{A}(\tau)$ has some (positive) eigenvalue diverging. An arbitrary flux configuration is expected to have F_1 components along the complete $\mathbb{A}(\tau)$ eigenbasis, so that for any diverging eigenvalue the flux part of $V(\varphi)$ diverges. As

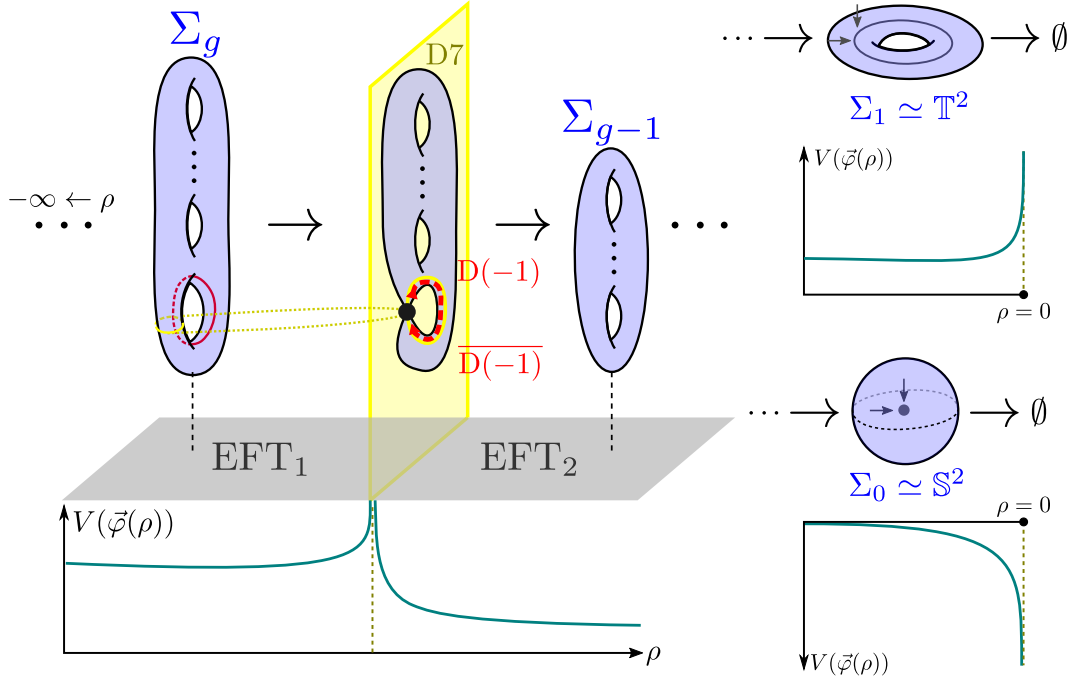


Figure 6. Sketch of different topology changes along the cobordism to nothing, depicting the intermediate losing of a handle for $g \geq 2$ (including the arrangement of the D7-domain walls, in yellow, and the $D(-1)$ - $D(-1)$ bounded on it, in red with a dashed line presenting the 1-chain joining them) and the two possible final topology changes into nothing, $\mathbb{T}^2 \rightarrow \emptyset$ and $\mathbb{S}^2 \rightarrow \emptyset$. The qualitative behavior of the scalar potential is also depicted.

is not needed that the cycle radius actually pinches to zero, as for $R \leq \sqrt{2\alpha'}$ (with α' the string tension) a tachyonic instability appears. This means that the $\Sigma_g \rightarrow \Sigma_{g-1}$ transition does not encounter an infinite potential barrier, but rather a finite-height slope up-hill until the instability region is reached and tachyon condensation occurs.

By inspection of action (4.14), it is evident that compactifying on Σ_g results in distinct low energy EFTs depending on the value of g , with the topology changes loci acting as domain walls between different theories. We will now comment on these changes occur as we move in the radial direction towards the end of the bordism to nothing. Assuming that the different topology changes are sufficiently separated from one another such that a lower $d = 8$ description is valid between them,

- The most evident feature of $\Sigma_g \rightarrow \Sigma_{g-1}$ is the change in the **scalar potential** $V(\vec{\varphi})$, as depicted in Figure 6. We first take the **internal curvature term**. Gauss-Bonnet theorem applied to compact Riemann surfaces result in this being proportional to $(g-1)$ times an extra $\mathcal{V}^{-4/3}$ factor coming from the rescaling to 8d Einstein frame. For $g \geq 2$ Σ_g are negatively curved, resulting in a runaway *positive* potential to large volume. At the

this happens for any 1-cycle pinching and the flux potential is non-negative, there must be some minimum in the bulk of the complex structure moduli space, resulting in their stabilization.

topology change locus a cycle pinches, with the overall volume of the internal manifold not being dramatically affected. Assuming that said volume remains approximately constant as we cross the domain wall (if our bordism \mathcal{B}_3 is smooth then this is the case), then the internal curvature contribution to the vacuum energy experiences a change of $\Delta V_{\mathcal{R}} \approx -\pi (\mathcal{V}/\mathcal{V}_0)^{-4/3} < 0$, with the change being energetically favored. For $g = 1$ (i.e. a torus compactification), there is no internal contribution to the curvature. If our bordism features an additional topology change to the sphere $\Sigma_0 = \mathbb{S}^2$, the curvature potential becomes negative. In this case the F_1 flux potential is 0, as there are no more 1-cycles, so there is no extra contributions to the potential (4.19). This drives $\mathcal{V} \rightarrow 0$, corresponding precisely to the $\mathbb{S}^2 \rightarrow \emptyset$ final topology change into nothing.

As for the **flux** contributions to the potential, apart from the overall $\mathcal{V}^{-4/3} e^\Phi$ factor driving towards a weak coupling and large volume limit there is the $\sum_{I=1}^{2g} Q^{I\top} \mathbb{A}(\vec{\chi}) Q^I$ factor. We can take the factorization approximation so that from (4.18),

$$\sum_{I=1}^{2g} Q^{I\top} \mathbb{A}(\vec{\chi}) Q^I \approx \frac{|\hat{\tau}|^2}{\hat{\tau}_2} Q^2 + \frac{1}{\hat{\tau}_2} Q'^2 + \sum_{I=3}^{2g} Q^{I\top} \mathbb{A}'(\vec{\chi}) Q^I, \quad (4.20)$$

where $\tau = \tau_1 + i\tau_2$ is the complex structure associated to cycle c pinching, Q and Q' the flux charges of that cycle and its dual (c'), and \mathbb{A}' the (4.17) matrix from the rest of factorized cycles. For $\tau_2 \rightarrow 0$ then the flux contribution to the potential grows, until the tachyon instability regime is reached and the topology changes occurs.

As for the units of flux lost in the topology change process, we must differentiate between those associated with the shrinking cycle c (Q) and those with its dual c (Q'). As was explained in sections 3.2 and 3.3, the shrinking of the cycle can be understood as a cobordism into nothing, with $\mathbb{S}^1 = \partial\mathbb{D}^2$. In order for this to be possible, we need a defect at the tip of the disk which eats up the charge. As reasoned in section 3.3, this corresponds to a D7-brane, magnetically charged under the C_8 form dual to C_0 . The (6+1)-dimensional topology change locus/domain wall (precisely where the flux potential naively would blow up) corresponds to the D7 brane, with the extra direction wrapped along the dual 1-cycle. This fixes the position of this intermediate D7 to be precisely at the topology change locus.

As for the charges associated to the dual 1-cycle, the topology change does not shrink it to nothing, but rather transforms it into a 1-chain with boundary. The total charge then must remain the same, with

$$Q' = \int_{c'} F_1 = \int_{\partial c'} C_0 = C_0|_{(\partial c')^+} - C_0|_{(\partial c')^-}. \quad (4.21)$$

We argue that this corresponds to a pair of $D(-1) - \overline{D(-1)}$ branes (D-instantons) localized on the D7 [115, 116], that are unstable and eventually annihilate each other, along with their charges. As a result these charges are not present at the other side of

the domain wall, and do not contribute to the potential anymore.

Under the factorization approximation the vacuum energy is lowered by

$$\Delta V_F \approx - \left(\frac{|\hat{\tau}^{(0)}|^2}{\hat{\tau}_2^{(0)}} Q^2 + \frac{1}{\hat{\tau}_2^{(0)}} Q'^2 \right), \quad (4.22)$$

with $\hat{\tau}^{(0)}$ the value of the pinching cycle complex structure before the topology change process starts. Again this is positive, so that the topology change process is energetically favored, both from the curvature and flux contributions to the vacuum energy.

- We now turn to the other term in the (4.14) action, corresponding to the gauge kinetic term for the resulting 2-form fields in the 8d EFT, $\mathcal{A}_{AB}(\vec{\varphi}) H_2^A \wedge \star H_2^B$, with $A = 1, \dots, 2g$. As explained in [114], for a 1-cycle c shrinking, with dual c' , both taken to be decoupled from the rest, we have that¹⁹

$$\begin{aligned} \mathbb{A}_{AB} H_2^A \wedge \star H_2^B &= \frac{\star 1}{\tau_2} |H_2^c - \tau H_2^{c'}|^2 + \dots \\ &= \frac{1}{\tau_2} |H_2^-|^2 + \tau_2 |H_2^+|^2, \end{aligned} \quad (4.23)$$

where $\tau = \tau_1 + i\tau_2$ is the factorized complex structure associated to c and c' and the (...) represent the kinetic terms for the forms not affected by the topology change. In the shrinking cycle limit $\tau_2 \rightarrow 0^+$, the combination $H_2^+ = H_2^c - \tau_1 H_2^{c'}$ becomes weakly coupled, while $H_2^- = H_2^{c'}$ becomes strongly coupled.

As the 1-cycle c shrinks along the bordism direction ρ in the topology change process, the 1-forms associated with the angular coordinate along c , $d\theta$, ceases to be harmonic, as the internal metric is warped with respect to ρ (i.e., \mathcal{B}_3 is no longer locally Σ_g times an interval). When decomposing $B_2 = B_1 \wedge d\theta$, close to the topology change locus $\Delta\theta \neq 0$, in such a way that the 8d field B_1 is massed-up and the $U(1)$ 1-form symmetry is removed from the EFT. At the same time, the angular profile θ of the condensing tachyon (B.2), which is wound along it, acts as a Goldstone boson of the broken $U(1)$ symmetry, see [76]. As for the gauge field associated to the dual c' , fundamental strings charged under the B_2 field and winding around c' in opposite directions are seen as charge-anticharge pairs from the (7+1)-dimensional point of view, charged under B_1^+ , where $H_2^+ = dB_1^+$. As $\tau_2 \rightarrow 0^+$, from (4.23) the gauge coupling of these grows stronger, with these pairs experimenting a strong attractive force (think of tension full flux string in 8d), until they encounter and annihilate each other. This results in the winding charge along c' to be effectively 0 as $\tau_2 \rightarrow 0$ and the $U(1)$ 1-form gauge symmetry is confined, thus not obstructing the handle decay. This is illustrated in Figure 7

¹⁹Note that there is a different sign and τ_2 factor in the expression when compared to that in [114], though the conclusions are the same.

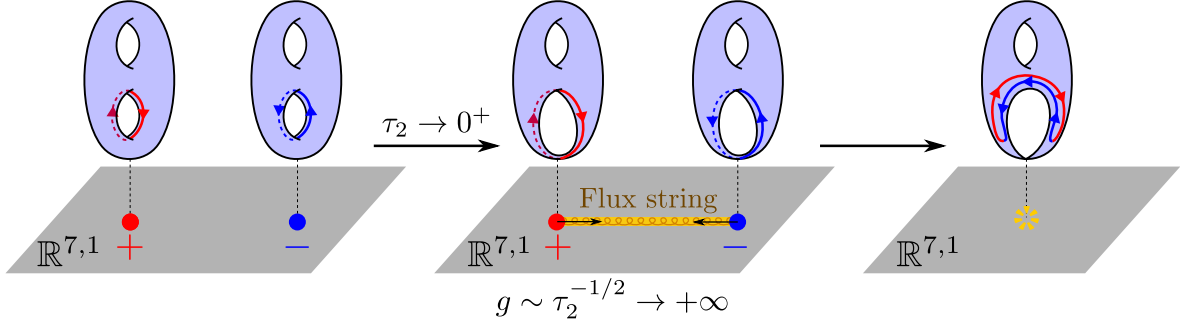


Figure 7. Sketch of the decay process of a handle in a $\Sigma_g \rightarrow \Sigma_{g-1}$ topology change, and the fate of the gauge $U(1)$ gauge form associated to the dual cycle, through confinement as the gauge coupling grows.

In the new EFT resulting on the other side of the topology change domain wall, the rank of the gauge group is two units lower, as the two $U(1)$ 1-forms associated to the two no-longer-present cycles have either been massed-up or classically confined [114], thus changing the gauge symmetry of the theory from $U(1)^{2g}$ to $U(1)^{2g-2}$.

While for simplicity we have considered only the dynamics of the $U(1)$ 1-form fields obtained from the integration of the B_2 field with one leg on the internal dimensions, analogous arguments could be done about 1- or 3-forms from doing the same with the C_2 and C_4 fields, respectively. Through each topology change, similar scenarios of massing-up/confining would arise.

In any case, we find that after any of the g or $g+1$ necessary topology changes in the bordism from Type IIB string theory on Σ_g to nothing, the vacuum energy lowers and the rank of the gauge group becomes smaller, with the different changes being energetically favored.

Before finishing this example, we briefly comment on the EotW brane picture of the above topology changes. These can be associated to global volume changing, parameterized by a canonically normalized volume modulus $\hat{\mathcal{V}} = \sqrt{2/3} \log \frac{\mathcal{V}}{\mathcal{V}_0}$, the canonically normalized 10d dilaton $\hat{\Phi} = \frac{1}{\sqrt{2}} \Phi$ appearing in the flux term, and the complex structure moduli, from which only the imaginary part of that corresponding to the shrinking cycle is of interest to us, $\hat{\tau}_2 = \frac{1}{\sqrt{2}} \log \tau_2$, where we have taken the factorization limit, see (A.10) in Appendix A. This allows us to approximate the scaling of the potential (4.19) as

$$V(\varphi) \sim e^{-2\sqrt{\frac{2}{3}}\hat{\mathcal{V}} + \sqrt{2}\hat{\Phi} + \sqrt{2}|\hat{\tau}_2|} \rightarrow \infty, \quad (4.24)$$

where we do not distinguish between the $\hat{\tau}_2 \rightarrow \pm\infty$ limits which are equivalent for the potential, and as we will see now not necessarily the three scalars simultaneously blow up. From our analysis, there are the following (qualitatively) different topology changes:

- $\Sigma_g \rightarrow \Sigma_{g-1}$: Here one of the 1-cycles shrinks to a point, i.e., $|\hat{\tau}_2| \rightarrow \infty$, while the overall volume is remains approximately constant. On the other hand, as we approach the

D7-brane, the dilaton goes to a weak coupling limit, $\hat{\Phi} \rightarrow -\infty$, see section 18.5 from [117]. This results in $V(\varphi) \sim \exp\left(\sqrt{2}\hat{\Phi} + \sqrt{2}|\hat{\tau}_2|\right)$, with critical exponent $\delta = 1$.

- $\Sigma_1 \simeq \mathbb{T}^2 \rightarrow \emptyset$: This case is analogous as the previous one, with also a D7-brane as a cobordism defect, but now the shrinking of a 1-cycle over its dual is also associated to the total volume going to 0, with the potential being (4.24), and $\delta = \sqrt{\frac{8}{11}}$.
- $\Sigma_0 \simeq \mathbb{S}^2 \rightarrow \emptyset$: For this final case the sphere shrinks to a point, with the 1-fluxes no longer contributing to the potential, so that $V(\varphi) \sim e^{-2\sqrt{\frac{2}{3}}\hat{\Phi}}$. It is then straightforward that in this case $\delta = \sqrt{\frac{8}{3}}$.

This way, the different topology changes are associated with distinct critical exponents, so from the EFT point of view are associated with different EotW brane solutions. As all $\Sigma_g \rightarrow \Sigma_{g-1}$ topology changes qualitative look the same, it is not possible, at least with this approach, to learn about the possible additional topology changes that the internal manifold must undergo after the first domain wall is crossed.

4.3 An example of non-minimal bordism

In the previous two examples studied, the bordisms considered saturated the Morse-Bott (3.13) and \mathcal{B}_{n+1} homology (3.8) inequalities, in such a way that the number of topology changes was minimized to only those unavoidable. There are, however, some results in the literature in which smooth bordisms which are non-minimal, i.e., those inequalities are fulfilled but not saturated. One of such examples was commented upon in Figure 5b and section 3.3, [107]. For a more detailed instance, we will comment on the BoN construction described in [30], whose relevant ingredients we review now. The following D -dimensional (bosonic) effective action is considered, which for simplicity we present in string frame²⁰

$$S_D^{(s)} = \frac{1}{2\kappa_D^2} \int d^D x \sqrt{-G} e^{-2\Phi} \left\{ \mathcal{R} + 4(\partial\Phi)^2 - \frac{1}{2 \cdot 3!} |H_3|^2 + \frac{1}{8} \alpha \mathcal{R}_{\text{GB}}^2 \right\}, \quad (4.25)$$

where Φ is the D -dimensional dilaton, $H_3 = dB_2$ and $\mathcal{R}_{\text{GB}}^2 = \mathcal{R}^2 - 4R_{MN}R^{MN} + R_{MNPQ}R^{MNPQ}$ is the Gauss-Bonnet invariant, which is topological for $D = 4$ and gives second-order e.o.m. for higher D . For $\alpha > 0$ both SUSY and the Dominant Energy Condition are broken. See [30] for more details on the embedding of the above action in $D = 6$ heterotic and the dual type I/IIB duals.

The above effective action can be further compactified to $d = 3$ on a 3-torus $\mathcal{C}_3 = \mathbb{T}^3$ with SUSY preserving (i.e., periodic) boundary conditions. The bordism structure considered is $\mathfrak{g} = \text{Spin}$, and since $\Omega_3^{\text{Spin}} \simeq 0$ [40, 67], there exists a Spin manifold \mathcal{B}_4 with $\mathcal{C}_3 = \partial\mathcal{B}_4$, and thus from the discussion in section 2.1 BoN constructions should exist. Due to the Spin

²⁰The Gauss-Bonnet invariant $\mathcal{R}_{\text{GB}}^2$ transforms in a pretty involved way under the conformal rescaling required to move to Einstein frame, see eq. (III.4) from [118]. As we will not make use of the actual equations of motion, we simply present the effective action in order to present the field content.

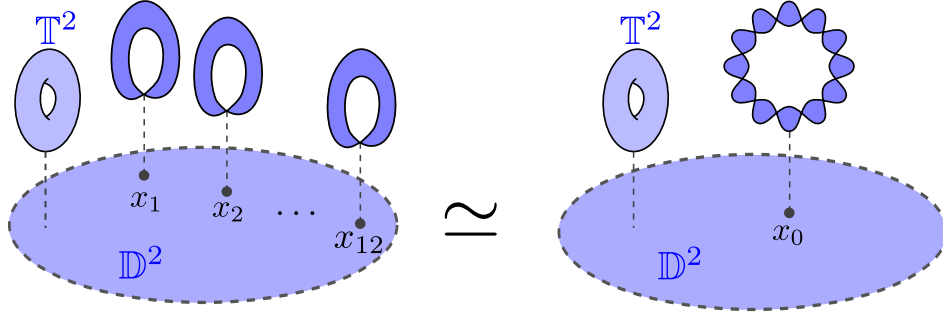


Figure 8. Sketch of the smooth fibration structure of $\mathbb{T}^2 \hookrightarrow \mathcal{B}_4 \rightarrow \mathbb{D}^2$, with the \mathbb{T}^2 fiber pinching at 12 points $\{x_i\}_{i=1}^{12}$. Considering the topology, the manifold can be continuously deformed such that the fibration is everywhere \mathbb{T}^2 except for a point x_0 of the \mathbb{D}^2 base where it pinches 12 times.

structure on \mathcal{C}_3 , \mathcal{B}_4 cannot simply be $\mathbb{D}^2 \times \mathbb{T}^2$, as we cannot just contract one of the 1-cycles to a point. Without the need of including stringy Spin-defects, a smooth solution is precisely given in [30, 119], with \mathcal{B}_4 given by elliptic fibration over $\mathbb{C} \simeq \mathbb{D}^2$ such that the \mathbb{T}^2 -fiber pinches in 12 points over the disk. If these degeneration loci are isolated, then \mathcal{B}_4 is smooth. In Figure 8 a sketch of the \mathcal{B}_4 manifold is presented. By continuously deforming it such that the 12 pinching points occurs on the same point of the base \mathbb{D}^2 , we can easily obtain $\vec{b}(\mathcal{B}_4) = (1, 1, 12, 0, 0)$ (rather than $\vec{b}(\mathbb{D}^2 \times \mathbb{T}^2) = (1, 2, 1, 0, 0)$), with no torsion. Note that these Betti numbers fulfill but do not saturate the inequalities (3.8). In any case, Morse-Bott inequalities (3.13) are satisfied as

$$(1+t)R(t) = (1+t)^2 t^2 + 12t^2 + (1+t)^3 - (1+t+12t^2) \implies R(t) = 2t + 2t^2 + t^3 \in \mathbb{R}_{\geq 0}[t], \quad (4.26)$$

where both the 12 pinching points have index 2 and the center of \mathbb{D}^2 , where the 1-cycle closes over the \mathbb{T}^2 fiber, have index 2. Note that after each critical point, where a 1-cycle pinches and then grows again, the local topology of the solution is actually the same, \mathbb{T}^3 , so that no actual topology change occurs. In any case, these types of critical points also enter in the Morse-Bott (3.13) and \mathcal{B}_{n+1} homology (3.8) inequalities, with certainly the bordism into question being different than $\mathbb{T}^2 \times \mathbb{D}^2$.

As explained in great detail in [30], each of the 12 degeneration points can be locally seen as a Taub-NUT/KK monopole solution [120, 121], with the compact space smoothly pinching, so that could also consider this solution as a 12-centered BoN solution. Close to this degeneration points, there is a partial decompactification, with the elliptic fiber becoming large while the \mathbb{S}^1 basis shrinks (so that the overall volume remains finite). This results in an infinite distance limit in moduli space being proven.²¹ From the EotW brane approach from section 2.2, there is no potential here for it to blow-up, so that $a = 0$ and $V_0 = 0$, and the critical exponent is $\delta = 2\sqrt{\frac{d-1}{d-2}}$. Again we refer to the extensive work of [30] for the detailed

²¹As explained in section 5.2.2 from [30], the associated KK tower is vital to cancel an *a priori* divergence in the metric around the degeneration points, such that the BoN solution remains smooth.

expressions.

This example might feel a bit underwhelming, as it involves a topology for \mathcal{B}_4 much more complicated than $\mathbb{T}^2 \times \mathbb{D}^2$, motivated by having a smooth bordism rather than using stringy defects such as those mentioned in footnote 6. Given the topology of \mathcal{B}_4 , which as described in [30] is determined by requiring 12 degeneration points of the elliptic fiber over the \mathbb{D}^2 base, one can use Morse-Bott inequalities to show that

$$\#\{1\text{-cycle} \rightarrow \{\text{pt.}\}\} - \#\{2\text{-cycle} \rightarrow \{\text{pt.}\}\} + \begin{cases} 2(1-g) & \text{if } \mathbb{S}^1 \rightarrow \Sigma_g \text{ end} \\ 0 & \text{otherwise} \end{cases} = 1 - b_1(\mathcal{B}_4) + b_2(\mathcal{B}_4),$$

where we denote $A \rightarrow B$ as a cycle A shrinking over a critical locus B . For our example we have $1 - b_1(\mathcal{B}_4) + b_2(\mathcal{B}_4) = 12$, with only 12 1-cycles shrinking over points and a final shrinking $\mathbb{S}^1 \rightarrow \mathbb{T}^2 = \Sigma_1$, with no 2-cycles shrinking over a point. Note that, in this aspect, the number of critical points is the minimum needed, and other solutions to the above equations would result in a higher amount of them.

4.4 A small step towards smooth bordisms for K3 compactifications.

We end this section with a comment on the bordism structure for a more complicated internal manifold than the Riemann surfaces from section 4.2: the 4-dimensional K3 surface. Considering the $\mathfrak{g} = \text{Spin}$ structure, we have that $\Omega_4^{\text{Spin}} \simeq \mathbb{Z} \simeq \langle \text{K3} \rangle$ [67], this is, precisely generated by K3, which carries negative unit charge under the conserved current $J_{p_1} = \frac{1}{48} p_1(R) = \frac{1}{48 \cdot 8\pi^2} \text{tr}(R \wedge R)$, with p_1 the first Pontriaguin class of the curvature 2-form R . How this $U(1)$ symmetry is killed in different string theories is discussed in detail in [40], to which we refer for more details. For our purposes, type IIA/M-theory can be compactified on pin^+ -manifolds [122], on which the bordism is broken to $\Omega_4^{\text{Spin}} \simeq \mathbb{Z} \rightarrow \Omega_4^{\text{pin}^+} \simeq \mathbb{Z}_{16} \simeq \langle \mathbb{RP}^4 \rangle$, which is then broken by MO5-planes [123, 124]. As for type IIB string theory, this is partly broken by non-trivial elliptic fibrations in F-theory, while, as argued in [40], there must be some new, non-supersymmetric defect with spatial dimensionality 6 that kills the remaining the remaining class. In order to obtain *smooth bordisms*, we will assume that defects are located far from the tip of the bordism, in such a way that our K3 surface can be taken belong to the trivial class of the spin bordism. As in section 4.2, we will only care about flux potentials and the location of the branes needed to eat-up the associated charges.

Before this, it is necessary to obtain information about the topology of the bordism \mathcal{B}_5 with $\text{K3} = \partial\mathcal{B}_5$. As K3 has Poincaré polynomial $P_t(\text{K3}) = 1 + 22t^2 + t^4$ (i.e. we only have 2-cycles and the whole 4-manifold to shrink). Using (3.8) and (3.9) we find that any bordism \mathcal{B}_5 for it must have Betti numbers $\vec{b}(\mathcal{B}_5) = (1, \alpha, 11, \beta, 0, 0)$, with $\alpha, \beta \in \mathbb{Z}_{\geq 0}$. Without creating new cycles, we have that the following possible topology changes to **(A)** 2-cycles shrinking to a point, **(B)** a 2-cycle shrinking over a compact 2-cycle of genus g , and **(C)** a 4-cycle shrinking to a point. The last two possibilities make 4 internal dimensions disappear, and as such correspond to the final topology change. Respectively denoting the number of each type

by $a \in \mathbb{Z}_{\geq 0}$ and $b, c \in \{0, 1\}$, we will then have that the LHS in (3.12) reads as

$$\begin{aligned} \text{MB}_t^N(\rho) - \mathcal{P}_t(\mathcal{B}_5) &= (c+b)t^5 + (1+2bg)t^4 + (a+b-\beta)t^3 + 11t^2 - \alpha t \\ &= (1+t)\mathcal{R}(t). \end{aligned} \quad (4.27)$$

Now, in order for the above polynomial to be divisible by $1+t$, we need $a = 12 - c + 2b(g-1) + \alpha + \beta$, which results in

$$\mathcal{R}(t) = (b+c)t^4 + (1-b-c+2bg)t^3 + (11+\alpha)t^2 - \alpha t. \quad (4.28)$$

As $\mathcal{R} \in \mathbb{Z}_{\geq 0}[t]$, then $\alpha = 0$ (i.e. \mathcal{B}_5 does not have non-trivial 1-cycles), and as we need a single final change into nothing, $b+c=1$, so that $\mathcal{R}(t) = t^4 + 2bgt^3 + 11t^2$, with $a = 12 - c + 2b(g-1) + \beta$, resulting in a total number of $N = a+b+c = 12 + b(2g-1) + \beta \geq 11$ topology changes in our cobordism into nothing. The above inequality is saturated for $(b, c, g, \beta) = (1, 0, 0, 0)$. We thus conclude that it is not possible to build a smooth BoN/EotW brane solution that interpolates into nothing without intermediate topology changes.

There are at least 11 topology changes, of which all but the final one (i.e. at least 10) correspond to 2-cycles shrinking to a point, thus resulting in its disappearance and that of its Poincaré dual 2-cycle. As for the final topology change, there are two possibilities, as commented before:

1. $(b, c) = (1, 0)$: Assume that after the intermediate a topology changes in each of which two (dual) 2-cycles disappear we end up with a 4-manifold \mathcal{X}_4 with $\vec{b}(\mathcal{X}_4) = (1, 0, 2\gamma, 0, 1)$ before the final topology change into nothing. By similar arguments as above, this final bordism \mathcal{M}'_5 will have $\vec{b}(\mathcal{M}'_5) = (1, 0, \gamma, \beta', 0, 0)$ and by Morse-Bott inequalities $\gamma = 1 - 2g - \beta'$, with $\beta' \in \{0, 1\}$. This results in $g = 0$ and two additional cases:
 - (a) $\beta' = 0$: Then $\gamma = 1$ and $\mathcal{P}_t(\mathcal{X}_4) = 1 + 2t^2 + t^4 = (1+t^2)^2$, and as such can be seen as a fibration $\mathbb{S}^2 \hookrightarrow \mathcal{X}_4 \rightarrow \mathbb{S}^2$, such as one of the Hirzebruch surfaces H_n [125]. Note that these have different topological invariants for distinct values of n , so on general they would correspond with different topologies of \mathcal{B}_5 . We also have that $a = 10 + 2\hat{a}$, with the extra $2\hat{a} = \beta \geq 0$ topology changes corresponding to creation and disappearance of pairs of 2-cycles.
 - (b) $\beta' = 1$: Then $\gamma = 0$ and $\mathcal{P}_t(\mathcal{X}_4) = 1 + t^4$, so \mathcal{X}_4 is an homology sphere. Again these are not unique [126], and could give rise to different bordism topologies. There will be $a = 11 + 2\hat{a}$, with additional $2\hat{a} = \beta - 1 \geq 0$ topology changes corresponding to additional creation and disappearance of pairs of 2-cycles.
2. $(b, c) = (0, 1)$: As in the previous case, after the a topology changes, our final 4-manifold before going to \emptyset has $\vec{b}(\mathcal{X}_4) = (1, 0, 2\gamma, 0, 1)$. Now in this case we have that \mathcal{X}_4 shrinks to a point as the boundary of \mathcal{M}'_5 with $\vec{b}(\mathcal{M}'_5) = (1, 0, \gamma, \beta', 0, 0)$. From Morse-Bott inequalities we have $\gamma + \beta' = 0$, and both numbers must be non-negative, we have

$\gamma = \beta' = 0$, so that \mathcal{X}_4 is a homology 4-sphere that shrinks to a point. As before, we will have $a = 11 + 2\hat{a}$, with the extra $2\hat{a} = \beta \geq 0$ again corresponding to creation and disappearance of pairs of 2-cycles.

To sum up, the minimal number of topology changes to go from a K3 compactification into nothing through a smooth bordism is either 11 or 12, respectively ending on a $\mathbb{S}^2 \hookrightarrow \mathcal{X}_4 \rightarrow \mathbb{S}^2$ fibration or a homology 4-sphere.

One could perform a similar analysis to that of section 4.2 to compactifications on K3. In this case, as $b_k(\text{K3}) = 0$ for odd k , only even fluxes contribute to the flux potential, so type IIA compactifications will be more interesting than type IIA, with D4- and wrapped D6-branes (with bound D2-branes from the dual 2-cycle) serving as domain walls between topology changes in the presence of flux along the whole K3 or the different 2-cycles. The analysis of the lower-dimensional gauge fields fate after topology change is analogous to those in section 4.2, so we will not comment on it further.

In section 7.2 of [107] a different bordism from K3 to nothing was argued for. F-theory on K3 (seen as a $\mathbb{T}^2 \hookrightarrow \text{K3} \rightarrow \mathbb{CP}^2$ fibration) is considered, which in Sen's weak coupling limit is dual to perturbative type IIB string theory on a $\mathbb{T}^2/\mathbb{Z}_2$ orbifold. The four resulting singularities, which are specified by the monodromy of a linking circle, are argued to be equivalent to four \mathbb{T}^2 with the same monodromy. This motivates the substitution of $\mathbb{T}^2/\mathbb{Z}_2$ by these genus-4 surface, which now allows for a smooth bordism to nothing as in section 4.2, and over which the F-theory elliptic fiber does not degenerate. The problem comes in that the process $(\mathbb{T}^2 \hookrightarrow \text{K3} \rightarrow \mathbb{CP}^2) \rightarrow (\mathbb{T}^2 \hookrightarrow \mathcal{X}_4 \rightarrow \Sigma_4)$ is not necessarily smooth, with this \mathcal{X}_4 , which contains non-trivial 1-cycles, not being required as an intermediate step of the analysis considered previously in this subsection. Since the construction of a completely smooth bordism to nothing for K3 compactifications (which for F-theory constructions need to keep the elliptic fibration until the final topology change into nothing) is not yet a solved matter, we hope this short digression serves to bring some light into the matter.

5 Stories with more than one ending

In the above sections, only a single BoN/EotW brane was considered for each case. However, instances of multi-centered BoN solutions eventually colliding or networks of EotW branes intersecting are the natural generalization. These cases have been previously studied in the literature (see [127–130] and [98, 99, 102], respectively), and as we will see, we can learn important qualitative properties through our approach.

5.1 Seeing double: Collisions of BoN's

As explained in section 2.1, bubbles of nothing have some non-zero probability of nucleating per unit volume. It is then expected, that, in a large macroscopic region and for a long enough period of time, several BoN nucleate and start growing, eventually approaching each other's surfaces. Considering our lower-dimensional theory to result from compactification on

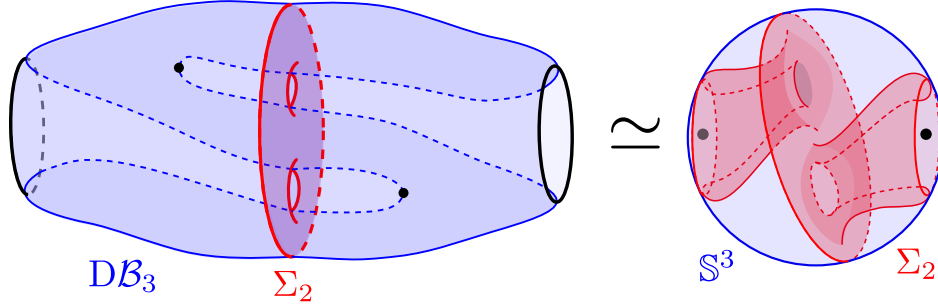


Figure 10. Illustration on how the double $D\mathcal{B}_3$ of the minimal bordism \mathcal{B}_3 of the genus-2 Riemann surface Σ_2 is diffeomorphic to the 3-sphere \mathbb{S}^3 , where Σ_2 is now seen as a submanifold. While each of the individual bordisms have two critical point loci, the resulting closed manifold has simply two critical points, required to be able to shrink it to a point. It is easy to see that the same type of deformations apply to arbitrary genus Riemann surfaces.

which implies

$$\sum_{k=0}^{n+1} (-1)^k [b_k(\mathcal{X}_{n+1}) - b_k(\mathcal{B}_{n+1}) - b_k(\mathcal{B}'_{n+1}) + b_k(\mathcal{C}_n)] = 0 \quad (5.4a)$$

$$\sum_{k=0}^{n+1} (-1)^k [t_k(\mathcal{X}_{n+1}) - t_k(\mathcal{B}_{n+1}) - t_k(\mathcal{B}'_{n+1}) + t_k(\mathcal{C}_n)] = 0. \quad (5.4b)$$

In the absence of torsion (i.e., all $t_k(\mathcal{M}) \equiv 0$), a homology sphere solution $\vec{b}(\mathcal{X}_{n+1}) = \vec{b}(\mathbb{S}^{n+1})$ is compatible²² with the above (5.2) and (5.4) equations, by choosing²³ $\mathcal{B}'_{n+1} \simeq \mathcal{B}_{n+1}$ and saturating (3.8). This is illustrated for $\mathcal{C}_2 \simeq \Sigma_2$ in Figure 10. This means that on principle there should not be a topological obstruction to the collision of two BoN with the \mathcal{X}_{n+1} compact manifold between them shrinking to a point.

However, in the presence of torsion, its coefficients and Poincaré duality do not align, and through (3.14) additional critical points in which topology change occurs are needed. As an example, consider the Lens space $\mathcal{C}_3 = L(p, q)$ from section 3.1, with $\vec{b}(\mathcal{C}_3) = (1, 0, 0, 1)$ and $\vec{t}(\mathcal{C}_3) = (0, 1, 0, 0)$. The bordism saturating (3.8) has $\vec{b}(\mathcal{B}_4) = (1, 0, 0, 0, 0)$ and $\vec{t}(\mathcal{B}_4) = (0, 1, 0, 0, 0)$. Applying then (5.3) results in $\vec{b}(\mathcal{B}'_4) = (1, 0, 0, 0, 0)$ and $\vec{t}(\mathcal{X}_4) = (0, 1, 1, 0, 0)$. From (3.14) a total of at least 6 critical points are needed, with $m_4 \geq 1$, $m_3 \geq 1$, $m_2 \geq 2$, $m_1 \geq 1$ and $m_0 \geq 1$, which means that the \mathcal{X}_4 manifold cannot shrink into a point without intermediate topology changes, which as previously stated can result in Planckian curvatures.

As a final comment, we note that, unlike in the case of a single BoN, which required the presence of $D(8 - p)$ -branes as cobordisms defects when considering p -form fluxes, here their presence is much more mild than the intermediate topology changes commented above.

²²Note that this does not imply such solution *exists*, but rather that there is no immediate obstruction to its existence.

²³For this choice, the resulting $D\mathcal{B}_{n+1} \simeq (\mathcal{B}_{n+1} \cup \overline{\mathcal{B}_{n+1}}) / \sim_{\partial\mathcal{B}_{n+1}}$ is called *double of \mathcal{B}_{n+1}* .

$D(8 - p)$ -branes, located along \mathcal{B}_{n+1} and \mathcal{B}'_{n+1} , needed to kill the p -form charges, have opposite orientations, and thus will annihilate each other when they collide as \mathcal{X}_{n+1} closes. Another way to see this is by considering that the (co)homology groups of \mathcal{X}_{n+1} and \mathcal{C}_n are different, and as commented above, $H_k(\mathcal{X}_{n+1}, \mathbb{Z}) \simeq H^k(\mathcal{X}_{n+1}, \mathbb{Z})$ can be trivial for $k = 1, \dots, n$ in the absence of torsion, meaning that the number of p -form fields/charges is no longer conserved on the compact manifold connecting the two BoN.

Going back to the non-minimal T^3 bordism in section 4.3, as explained in [30], $\partial\mathcal{B}_4$ can be thought as “half a K3” manifold, understood as an elliptical fibration over a \mathbb{P}^1 base, with 24 degenerations. This way, the double of our bordism is indeed $D\mathcal{B}_4 = K3$, which is not a homology 4-sphere, and as such, cannot be shrunk to a point without intermediate topology changes. The collision of two BoN such as those described in [30] would require Planckian curvatures and stringy effects, even if these were not needed for the single BoN construction.

5.2 Going a bordism further: Intersection of EotW branes

We finally consider the cases with more than one bordism to nothing, in the language of EotW branes. Intersection of these was studied in [98, 99, 102], and in this section we will study them from the point of view of topology changes between “cobordant” bordisms to nothing.

From the EFT point of view, the single EotW brane from section 2.2 was generalized to k intersecting EotW branes in [98]. For this the following lower- d EFT action is considered,

$$S = \frac{1}{2} \int d^d x \sqrt{-g} \left\{ \kappa_d^2 [\mathcal{R}_g - G_{ij} \partial_\mu \phi^i \partial^\mu \phi^j] - 2V(\vec{\phi}) \right\} , \quad (5.5)$$

where the moduli space metric has unit diagonal, $G_{ii} = 1$, as well as the following ansatz for a conformally flat metric (see [102] for EotW solutions with non-conformally flat backgrounds):

$$ds_d^2 = e^{-2\sum_{i=1}^k \sigma_i} ds_{d-k}^2 + \sum_{i=1}^k e^{-2\sum_{j \neq i} \sigma_j} (dy^i)^2 + f_{ij} e^{-\sigma_i - \sigma_j} dy^i dy^j . \quad (5.6)$$

with $\phi^i = \phi^i(y^i)$ and $\sigma_i = \sigma^i(y^i)$ and each EotW brane located at $y^i = 0$. The f_{ij} metric term is taken to be constant and such that no pair of branes become (anti)parallel (what would result in a degenerate metric). In the same way as in section 2.2, the potential, metric and scalars have a universal behavior,

$$V(\vec{\phi}) = \sum_{i=1}^k V_{i,0} e^{\delta_i \phi^i + \sum_{j \neq i} a_j \delta_j \phi^j} , \quad \text{with } G_{ij} = \sqrt{a_i a_j} \quad (5.7a)$$

$$\phi^i(y^i) = -\frac{2}{\delta_i} \log y^i , \quad \sigma_i(y^i) = -\frac{4}{(d-2)\delta_i^2} \log y^i . \quad (5.7b)$$

When moving towards $y^i \rightarrow 0$ with the other coordinates fixed, ϕ^i scales as if approaching a single EotW brane, eventually exploring a specific limit of moduli space. Different spacetime

trajectories when approaching the EotW brane network result in other trajectories along the asymptotic regimes in moduli space. The off-diagonal values of G_{ij} and f_{ij} depend on the specific construction of the EotW brane intersection.

As explained in [98], the intersection of two EotW branes can be understood as providing a boundary to the theory living on each of the (possibly different) branes, or, more in line with the interpretation we will give now, as domain walls between the different boundaries of the theory.

From the point of view of Morse-Bott theory and the possible topologies of bordisms introduced in section 3, intersecting EotW branes have a very natural reading. We can understand different EotW solutions as having either distinct Morse functions $\rho : \mathcal{B}_{n+1} \rightarrow [0, +\infty)$ on the same \mathcal{B}_{n+1} (note that ρ can be directly read from the metric and thus is determined by a solution to the equations of motion), or simply by bordisms to nothing with $\mathcal{B}_{n+1} \not\cong \mathcal{B}'_{n+1}$. These different bordisms feature different topology changes, either in nature or order, and thus from the EFT point of view have different scalars blowing up, with unrelated critical exponent, determined by the first topology change.

In the presence of n compact dimensions, we can understand the intersection of an arbitrary number $k < d$ of EotW branes from the perspective of k -categories [131, 132]. From a categorical point of view, the bordisms on n -manifolds define a category $\mathbf{Cob}(n+1)$ in the following way:

- Elements of $\mathbf{Cob}(n+1)$ are closed and oriented n -manifolds.
- Given $\mathcal{M}_n, \mathcal{N}_n \in \mathbf{Cob}(n+1)$, a bordism \mathcal{B}_{n+1} for them defines a morphism $\mathcal{B}_{n+1} : \mathcal{M}_n \rightarrow \mathcal{N}_n$ in $\mathbf{Cob}(n+1)$. Two bordisms \mathcal{B}_{n+1} and \mathcal{B}'_{n+1} define the same morphism in $\mathbf{Cob}(n+1)$ if there is an orientation preserving diffeomorphism $\mathcal{B}_{n+1} \simeq \mathcal{B}'_{n+1}$ extending that of their boundaries, $\partial\mathcal{B}_{n+1} \simeq \partial\mathcal{B}'_{n+1} \simeq \mathcal{M}_n \sqcup \overline{\mathcal{N}}_n$.
- Given $\mathcal{M}_n \in \mathbf{Cob}(n+1)$, the identity morphism $\text{id}_{\mathcal{M}}$ is given by $\mathcal{I}_{n+1} = \mathcal{M}_n \times [0, 1]$.
- Composition of morphisms is given by gluing morphisms together by their intermediate boundary.

We can use this notion to define the k -category $\mathbf{Cob}_k(n+k)$ recursively, by setting $\mathbf{Cob}(n+1) = \mathbf{Cob}_1(n+1)$, and defining $\mathbf{Cob}_2(n+2)$ as follows:

- The elements of $\mathbf{Cob}_2(n+2)$ are closed oriented manifolds of dimensions n .
- Given $\mathcal{M}_n, \mathcal{N}_n \in \mathbf{Cob}_2(n+2)$, the category $\mathcal{C} = \text{Map}_{\mathbf{Cob}_2(n+2)}(\mathcal{M}_n, \mathcal{N}_n)$ is given by the bordisms from \mathcal{M}_n to \mathcal{N}_n , this is, the oriented $(n+1)$ -manifolds \mathcal{B}_{n+1} such that $\partial\mathcal{B}_{n+1} = \mathcal{M}_n \sqcup \overline{\mathcal{N}}_n$. Now, given $\mathcal{B}_{n+1}, \mathcal{B}'_{n+1} \in \mathcal{C}$, $\text{Hom}_{\mathcal{C}}(\mathcal{B}_{n+1}, \mathcal{B}'_{n+1})$ is the collections of bordisms \mathcal{X}_{n+2} from \mathcal{B}_{n+1} to \mathcal{B}'_{n+1} , reducing to the trivial bordism along their common boundary $\partial\mathcal{B}_{n+1} = \partial\mathcal{B}'_{n+1} = \mathcal{M}_n \sqcup \overline{\mathcal{N}}_n$, in such a way that

$$\partial\mathcal{X}_{n+2} \simeq \mathcal{B}_{n+1} \cup [(\mathcal{M}_n \sqcup \overline{\mathcal{N}}_n) \times [0, 1]] \cup \overline{\mathcal{B}'_{n+1}}. \quad (5.8)$$

In other words, we consider bordisms between bordisms. It can be shown (see [132] for more details and some nuances in the definitions) that the above structures are well-defined, and as such $\text{Hom}_{\mathcal{C}}(\mathcal{B}, \mathcal{B}') \neq \emptyset$, so that two bordisms of the same manifolds are always cobordant.

For our purposes, we will restrict $\mathbf{Cob}_2(n+2)$ to consist in $\{\mathcal{C}_n, \emptyset\}$, with the empty set seen as a n -dimensional manifold, such that $\mathcal{C} = \text{Map}_{\mathbf{Cob}_2(n+2)}(\mathcal{C}_n, \emptyset)$ are the possible bordisms from our compact manifold to nothing. Each of this will correspond to a different EotW brane/BoN construction. Finally, the elements in $\text{Hom}_{\mathcal{C}}(\mathcal{B}_{n+1}, \mathcal{B}'_{n+1})$ will be the bordisms between this, interpolating between intersecting EotW branes. An “angular” coordinate θ parallel to the two branes and perpendicular to the radial one ρ can act as a new Morse-Bott function over $\mathcal{X}_{n+2} \in \text{Hom}_{\mathcal{C}}(\mathcal{B}_{n+1}, \mathcal{B}'_{n+1})$. Following an analogous procedure to that of section 3, one could bound the topology of \mathcal{X}_{n+2} , and from that, the topology changes in going from \mathcal{B}_{n+1} to \mathcal{B}'_{n+1} , which can be then understood as the intersecting EotW branes. As the necessary defects to kill topological/cobordism charges should be the same, on principle no additional defects would be needed to be located at these intersections/topology changes (a feature also observed in the universal scalings studied in [98]), with \mathcal{B}_{n+1} and \mathcal{B}'_{n+1} differing only on their arrangement. See Figure 11 for a simple example in a toroidal compactification. This analysis could on principle allow us to obtain the qualitative properties and topological structure of intersecting EotW branes, which so far have not been thoroughly explored, though explicit examples appear in [98].

To illustrate the above reasoning, we consider a network of EotW branes in the type IIB on Σ_g from section 4.2. For simplicity, we take $\Sigma_1 \simeq \mathbb{T}^2$. There are two possible bordisms that do not imply the creation of new cycles, namely **(A)** the shrinking of one cycle over its dual such that $\mathcal{V} \rightarrow 0$ and the torus goes to nothing in a single step, and **(B)** the pinching of a cycle, such that there is a topology change to \mathbb{S}^2 , which later shrinks to a point. As discussed below (4.24), these two bordisms are associated to distinct critical exponents, $\delta_{\mathbf{A}} = \sqrt{\frac{8}{11}}$ and $\delta_{\mathbf{B}} = 1$. If the original \mathbb{T}^2 is threaded by F_1 flux, then this domain wall (which in **(A)** ends spacetime) corresponds with a D7-brane wrapped along the dual 1-cycle. This is illustrated in Figure 11. The angle $\alpha > 0$ between the different EotW branes should be set by the tension of the unknown object/defect that causes the Morse-Bott function to have different critical points as we move in the parallel direction θ . Understanding its nature would allow us to compute the value of said angle.

Seeing $\{\text{Crit}(\rho)|_{\theta}\}_{\theta}$ as a set parameterized by θ (for the case shown in Figure 11 this is not even a manifold), the point θ_* where the fiber changes topology correspond with the location of the EotW branes intersection.

From Figure 11, it is easy to visualize analogous EotW branes to **A** and **B** given by the bordisms associated to the shrinking/pinching of cycles duals to those presented in Figure 11. Connecting the different possibilities, one could find a network

$$\dots \longleftrightarrow \text{EotW}_{\mathbf{A}} \longleftrightarrow \text{EotW}_{\mathbf{B}} \longleftrightarrow \text{EotW}_{\mathbf{A}'} \longleftrightarrow \text{EotW}_{\mathbf{B}'} \longleftrightarrow \dots$$

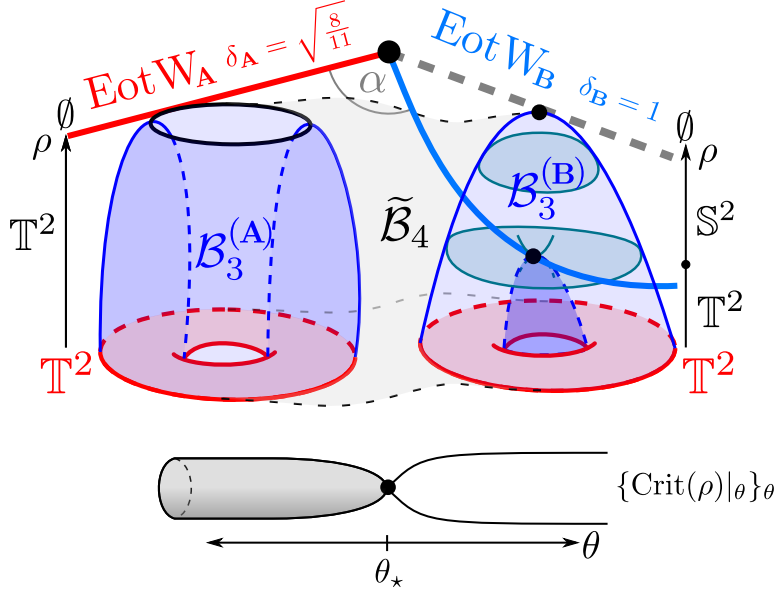


Figure 11. Illustration of the intersection of two EotW branes of a $\mathcal{C}_2 = \mathbb{T}^2$ compactification, respectively associated to shrinking of a 1-cycle over its dual (**A**), and of said 1-cycle over a point (**B**), resulting in a topology change $\mathbb{T}^2 \rightarrow \mathbb{S}^2$ before the final shrinking of this to nothing. These two possibilities are described in section 4.2, and up to the EotW brane surface, they both share the same EFT description. The set $\{\text{Crit}(\rho)|_\theta\}_\theta$ is also depicted, being topologically \mathbb{S}^1 for EotW_{**A**} and two points for EotW_{**B**}. The transition between the two corresponds to the EotW branes intersection. The associated critical exponents are also depicted.

as we move in the θ direction. A single type of defect would be enough to explain the same angle α between the branes at each intersection. Identifying its nature and the value of α could allow us to put an upper bound on the number of possible EotW branes, as these could not span more than the celestial sphere. See [98] for other explicit computations of the critical exponents in EotW brane intersection networks for compactifications on Calabi-Yau threefolds.

The above reasoning can be extended to intersections of more than two EotW branes. For this we recursively define $\mathbf{Cob}_k(n+k)$ (restricted to $\{\mathcal{C}_n, \emptyset\}$), progressively trading spatial directions with coordinates (acting as Morse-Bott functions) in the higher-dimensional bordism. The end point of these sequence of k -categories is given by $\mathbf{Cob}_{d-1}(d+n-1)$, where every spatial macroscopic direction is capped by an EotW brane, resulting in a (spatially) finite-volume universe. This might be of interest in the context of “Bubbles of something” and the “boundary proposal” [77, 79], see also [133–136], where the universe is nucleated by the reverse process of a bubble of nothing, in such a way that the boundary of these gravitational instantons could be described by local patches of different topology. In any case, we will not comment more on this and leave it for a future work.

6 Conclusions and Outlook

In this paper, we have given a new interpretation of spacetime bordisms to nothing through Morse-Bott theory. The radial distance to the end of spacetime is interpreted as a Morse function over the bordism and its fibers or level curves correspond to the internal manifold at each spacetime point. We are thus able to obtain properties of the internal topology changes for bordisms to nothing admitting a topological manifold description, learning about which of these changes must always occur, and where defects, such as Dp -branes, must be located. Though qualitative in nature, these results serve as a first step towards a piece-wise construction of spacetime ending configurations, such as BoN solutions, for more involved internal geometries. Knowing their topology, it might be possible proceed analogously to [30], dividing \mathcal{B}_{n+1} into different regions whose metric can be given an analytic approximate expression, and later gluing them together. As happens with the analysis in section 4.2, for large volume regimes in \mathcal{C}_n it is consistent to expect that topology changes on the compact manifold, consisting in the shrinking of some internal cycles, do not immediately trigger topology changes for the rest of cycles. This way it is possible to have an EFT description between the different domain walls.

Furthermore, we are able to extend our results and interpretation to more involved settings such as collision of Bubbles of Nothing, where we identify the possible existence (or lack) of topological obstructions resulting in curvature singularities before the tip of the BoN come into contact. We also provide an interpretation of the intersection of EotW branes through higher bordisms, which might help in the understanding of the junction structure.

Our results are only a first step, however. The new findings are mostly in the topological, more qualitative, side of the bordisms to nothing. While in section 4.2 we commented on how, for type IIB compactifications on Σ_g each topology change lowered the value of the vacuum energy, in general one would like to also obtain the decay rates associated to them, in line with the examples in [30] and the general considerations on decay rates/nucleation probabilities on bubbles of nothing/something from [77, 79]. Smooth bordisms are interesting precisely for this purpose, as their action can be computed directly with EFT ingredients, without the need to include UV contributions whose behavior might not be well understood, and also diverge from the EFT perspective. One could expect that the different types of topology changes could be studied separately, in such a way that by considering the different chains (3.1) $\mathcal{C}_n = \mathcal{C}_n^{(0)} \rightarrow \mathcal{C}_n^{(1)} \rightarrow \dots \rightarrow \mathcal{C}_n^{(m)} = \emptyset$, with the total decay rate given as a sum of blocks associated to each of the changes, in such a way that different bordisms could be sorted by their decay rate. This would be interesting for obvious phenomenological reasons, but goes well over the scope of the paper, and it is left for future work.

Another matter is that of the defects considered. As commented above, for our approach to apply, we need to have smooth bordisms, or at most mild defects such as conical singularities which can be “smoothed out”. While cobordism defects such as Dp -branes fulfill this, and indeed we have been able to infer their arrangement along the bordism, other more singular

defects, such as O-planes, or more exotic branes [40, 137], might not guarantee that. It would be nice to understand which types of defects allow for some *smooth(able) manifold* description and which do not. As evidenced by the example from [137] shown in Figure 5b, some of these defects or configurations require for non-trivial cycles along \mathcal{B}_{n+1} (resulting in *thick* domain walls), and thus cannot be located along minimal bordisms. A general understanding of when more involved bordisms are required would also have important implications for the construction of realistic BoN.

Apart from topological constraints, we have not considered the possible dynamical restrictions to vacuum decay. It is possible that, in the process of breaking some of them, specific decay channels or bordism topologies are singled-out or excluded. We leave for a future project the better understanding of the relation between these dynamical constraints and processes through which the topology/geometry of \mathcal{B}_{n+1} changes. On the other hand, as explained in Appendix B and [113, 114], topology changes consisting in the decay of a 1-cycle can be explained through tachyon condensation. One expects that tachyon condensation is also involved in decay of higher dimensional cycles, but the explicit mechanism does not directly translate from the 1-cycle case. The worldsheet interpretation of n -cycle closing is an interesting problem we would like to return to in the future.

Other type of restrictions would be those in which a fibration structure is required along the complete bordism direction. For example, F-theory compactifications need to keep the elliptic fiber for all values of ρ , and thus \mathcal{B}_{n+1} , with topology changes in which said fiber disappears not being considered. A possible solution would be trying to extend the $\mathbb{T}^2 \hookrightarrow \mathcal{C}_n \rightarrow \mathcal{D}_{n-2}$ fibration to $\mathbb{T}^2 \hookrightarrow \mathcal{B}_{n+1} \rightarrow \hat{\mathcal{D}}_{n-1}$, in such a way that $\partial\hat{\mathcal{D}}_{n-1} = \mathcal{D}_{n+2}$ and the bordism fibration restricting to that of \mathcal{C}_n along the boundary. How to properly perform this is beyond the scope of this paper.

As commented in section 3, we have made use of two sets of inequalities relating the topology of the bordism \mathcal{B}_{n+1} with the number and type of topology changes/critical points experienced, namely *Morse-Bott inequalities for manifolds with boundary* (not including torsion) (3.12) and *Morse inequalities (including torsion) for manifolds without boundary* (3.14). As the former does not include torsion, while the later requires $\partial\mathcal{M} = \emptyset$ and only consider critical points rather than general submanifolds, their range of applicability is different. Ideally one would like to incorporate torsion into (3.12), but as far as we know this is not present in the mathematics literature. On the other hand, while (3.12) apply also when the compactification manifold \mathcal{C}_n has a non-zero boundary, it would be interesting to obtain a generalization of the bounds (3.8) on the topology of the bordism for cases other than $\partial\mathcal{C}_n = \emptyset$, as this was an assumption that was needed in their derivation.

It has been conjectured [138, 139] that Calabi-Yau threefolds always admit a \mathbb{T}^3 fibration, what motivated the authors in [30] to propose that the BoN solutions constructed for spin bordisms on this manifold (see also [140] for the additional bordisms of \mathbb{T}^3 to nothing) could be used as decay channels for realistic CY_3 compactifications. However, as we have shown with examples such as precisely $\mathbb{T}^2 \hookrightarrow \mathcal{B}_4 \rightarrow \mathbb{D}^2$ bordism for \mathbb{T}^3 in section 4.3, bordisms

given by non trivial fibrations have different homology groups than their trivial counterparts, resulting in a different topology change sequence. While the claim of [30] probably holds in the sense that an analogous decay channel exists, it is not immediate that the constructions known in the literature can be straightforwardly used, as the \mathbb{T}^3 fibration might not be trivial.

Although we have simply considered the ρ component of the bordism metric as our Morse function, it is easy to see that any p -form field ω defined on \mathcal{C}_n can be extended into the whole bordism \mathcal{B}_{n+1} as a $(p+1)$ -form by taking $\omega' = \omega \wedge d\rho$, being zero at critical points of ρ . It might be interesting to relate general properties of these fields with those of the bordism. Furthermore, we would like to point out that only (co)homology coefficients such as Betti numbers and torsion ranks have been considered. We leave for future work the possibility of recovering other topological invariants of the bordism from those of \mathcal{C}_n , as well as understanding to which dynamical properties of the bordism to nothing they are related to.

There is still much to be understood and computed about the possible channels through which our universe can decay to nothing. Computations are usually quite involved, so that apart from specific cases [30], most constructions in the literature feature relatively simple compactifications. We believe that studying more complicated cases can lead to a better understanding of how our universe can be created and disappear into nothing is within reach, and we expect this paper serves as a small step in this direction.

Acknowledgments: We are very grateful to Matilda Delgado, Miguel Montero and Irene Valenzuela for their invaluable contributions through extensive discussions and comments on the manuscript. We would like to also thank Alberto Castellano, Markus Dierigl, Bjoern Friedrich, Arthur Hebecker, Jesús Huertas, Andriana Makridou, Luca Melotti, Jacob McNamara, Jakob Moritz, Eduardo Velasco and Matteo Zatti for illuminating discussions and comments along the past two years. I.R. wishes to acknowledge the hospitality of the Depart of Theoretical Physics at CERN and the Department of Physics of Harvard University during different stages of this work. I.R. acknowledges the support of the Spanish FPI grant No. PRE2020-094163 and the ERC Starting Grant QGuide101042568 - StG 2021, as well as the Spanish Agencia Estatal de Investigación through the grant “IFT Centro de Excelencia Severo Ochoa” CEX2020-001007-S and the grant PID2021-123017NB-I00, funded by MCIN/AEI/10.13039/501100011033 and by ERDF “A way of making Europe”.

A Basics of Compact Riemann Surfaces

In this appendix we review the basic results about Riemann surfaces that are used in section 4.2. For our purposes, a (compact) genus- g Riemann surface Σ_g can be seen as the connected sum of g 2-torus $\mathbb{T}^2 = \mathbb{S}^1 \times \mathbb{S}^1$, $\Sigma_g := \#^g \mathbb{T}^2$, with $\Sigma_0 = \#^0 \mathbb{T}^2 \simeq \mathbb{S}^2$. Regardless of its genus, every compact Riemann surface Σ admits a conformal Riemann metric [141], i.e., $ds_\Sigma^2 = \lambda(z)^2 dz d\bar{z}$, with $\lambda \in \mathcal{C}^2(\Sigma)$ and $z = x + iy$. A simple computation yields that the Ricci

scalar is given by $\mathcal{R}_\Sigma = -2\Delta \log \lambda$, with $\Delta = \lambda^{-2}(\partial_x^2 + \partial_y^2)$. Given Γ a discrete subgroup of

$$PSL(2, \mathbb{R}) = \left\{ \begin{pmatrix} a & b \\ c & d \end{pmatrix} : ad - bc = 1 \right\}, \quad (\text{A.1})$$

acting discontinuously and without fixed points on the upper half plan $\mathbb{H} = \{z = x + iy \in \mathbb{C} : y > 0\}$, then $\Sigma = \mathbb{H}/\Gamma$ is a compact Riemann surface. Then, for an arbitrary $z_0 \in \mathbb{H}$, the set

$$F = \{z \in \mathbb{C} : d(z, z_0) \leq d(z, \gamma z_0) \forall \gamma \in \Gamma\}, \quad (\text{A.2})$$

where d is the geodesic distance associated to the natural hyperbolic metric $ds_{\mathbb{H}}^2 = \frac{dzd\bar{z}}{2\text{Im}(z)^2}$, is a convex polygon with finitely many sides, such that all the vertices are equivalent. It can then be shown [141] that sides of F can be paired $a \equiv a'$ uniquely, in such a way that the sides can be ordered as either $a_0 a'_0$ or $a_1 b_1 a'_1 b'_1 \dots a_g b_g a'_g b'_g$ in such a way that F has 2 or $4g$ sides. The fundamental group of Σ (which is obtained from F after sides are identified) is then

$$\pi_1(\Sigma) = 0, \quad \text{or} \quad \pi_1(\Sigma) = \langle \langle \{a_i, b_i\}_{i=1}^g \rangle : a_1 b_1 a_1^{-1} b_1^{-1} \dots a_g b_g a_g^{-1} b_g^{-1} = 1 \rangle, \quad (\text{A.3})$$

respectively. Being the abelianization of the fundamental group, the first homology groups are then

$$H_1(\Sigma; \mathbb{Z}) = 0, \quad \text{or} \quad H_1(\Sigma; \mathbb{Z}) = \mathbb{Z}^{2g}, \quad (\text{A.4})$$

respectively corresponding with $\mathbb{S}^2 = \Sigma_0$ or Σ_g .

For $g \geq 1$ we can take dual canonical homology and cohomology basis $\{a_i, b_i\}_{i=1}^g$ and $\{\alpha^i, \beta^i\}_{i=1}^g$ such that we have the following intersections and integrals [113]:

$$a_i \cdot a_j = b_i \cdot b_j = 0, \quad a_i \cdot b_j = -b_i \cdot a_j = \delta_{ij} \quad (\text{A.5a})$$

$$\int_{a_i} \beta^j = \int_{\beta_i} \alpha^j = 0, \quad \int_{a_i} \alpha^j = \int_{b_i} \beta^j = \delta^{ij}, \quad (\text{A.5b})$$

such that for any 1-form $\eta \in \Omega^1(\Sigma_g)$

$$\int_{a_i} \eta = \int_{\Sigma_g} \eta \wedge \beta^i, \quad \int_{b_i} \eta = \int_{\Sigma_g} \alpha^i \wedge \eta \quad (\text{A.6})$$

in such a way that one can expand any 1-form as $\eta = m_i \alpha^i + n_j \beta^j$. On the other hand, we can define a holomorphic basis $\{\omega^i\}_{i=1}^g$ with

$$\int_{a_i} \omega^j = \delta^{ij}, \quad \int_{b_j} \omega^j = \Omega^{jj}, \quad (\text{A.7})$$

where Ω is a symmetric matrix with positive definite imaginary part known as *period matrix*. One can show that Ω only depends on the homology classes of the 1-cycles, with the space of

period matrices, \mathbb{H}^g , having complex dimension $\frac{1}{2}g(g+1)$.

On the other hand, from the Riemann-Roch theorem [117, 141], one has that

$$\#\text{complex moduli parameters} - \#\text{conformal Killing vectors} = -\frac{3}{2}\chi(\Sigma_g) = 3(g-1), \quad (\text{A.8})$$

which we can study separately:

- For $\Sigma_0 = \mathbb{S}^2$, we have as metric $ds^2 = \frac{4dzd\bar{z}}{(1+|z|^2)^2}$, with 3 conformal Killing vectors, $\{z^a \partial_z\}_{a=0}^2$, resulting in no complex structure moduli (one must still consider the volume).
- For $\Sigma_1 = \mathbb{T}^2$, we have a flat metric $ds^2 = dzd\bar{z}$. The translations along the torus are given by $U(1) \times U(1)$, with a single complex generator, resulting in one conformal Killing vector and one complex moduli parameter, $\tau = \tau_1 + i\tau_2 \in \mathbb{H}$. As one considers the $SL(2, \mathbb{Z})$ redundancies, the actual fundamental domain is smaller and corresponding with the famous $\mathcal{F} = \{-\frac{1}{2} \leq \tau_1 \leq 0, |\tau|^2 \geq 1\} \cup \{0 < \tau_1 \leq \frac{1}{2}, |\tau|^2 > 1\}$.
- For $g \geq 2$ there are no conformal isometries, with the number of complex moduli parameters being $3g-3$. While for $g=2, 3$ this is the same as $\frac{1}{2}g(g+1)$, for $g \geq 4$ the Teichmüller space \mathcal{T}_g is embedded in \mathbb{H}^g in a non trivial way [141], so that no all choices of $\tau \in \mathbb{H}^g$ actually correspond to a complex structure in Σ_g . In any case, given Σ_g and its homology classes, τ is uniquely determined. In general, we will have the same problem of defining the fundamental region \mathcal{F}_g from \mathcal{T}_g , with [117]

$$\mathcal{F}_g = \frac{\mathcal{T}_g}{\text{Diff}/\text{Diff}_0}, \quad (\text{A.9})$$

where Diff are the diffeomorphisms of Σ_g and Diff₀ those connected to the identity. We will not develop further in this direction.

The different limits in which a handle degenerates and topology changes occurs are expected to be associated with one of the eigenvalues of Ω going to infinity or 0. In general, the explicit expression of the complex structure moduli space metric are quite involved and depend on the specific realization and global metric of Σ_g . However, as shown in Figure 12, we can approximate this by considering a handle of $\Sigma_g \simeq \Sigma_{g-1} \# \mathbb{T}^2$ effectively factorized from the rest, so that it can be seen as \mathbb{T}^2 , whose (constant volume) metric and complex structure moduli space are given by

$$g_{ab} = \tau_2^{-1} \begin{pmatrix} 1 & \tau_1 \\ \tau_1 & |\tau|^2 \end{pmatrix}, \quad G_{ij} \partial_\mu \varphi^i \partial^\mu \varphi^j \supseteq \frac{\partial_\mu \tau \partial^\mu \bar{\tau}}{2\tau_2^2} = \frac{(\partial\tau_1)^2}{2\tau_2^2} + \left[\partial \left(\frac{1}{\sqrt{2}} \log \tau_2 \right) \right]^2 \quad (\text{A.10})$$

The decay of said handle can be interpreted as a $\tau_2 \rightarrow 0, +\infty$ limit, which indeed are at infinite distance.

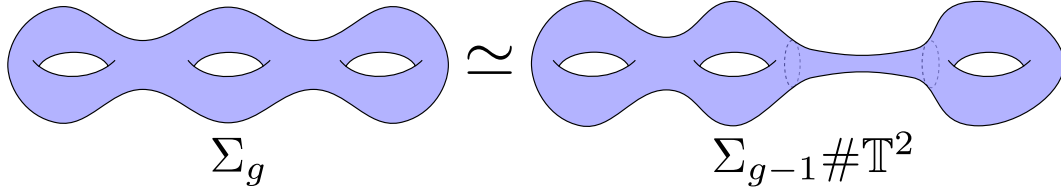


Figure 12. Illustration of how a handle of a Riemann surface Σ_g can be factorized from the main body by considering the connected sum of a torus \mathbb{T}^2 and a lower genus Σ_{g-1} , joined together by a thin tube. For large g the volume of the whole surface is approximately constant, and the dynamics of the handle decay should not affect those of the rest of the manifold. In this limit the factorized handle can be effectively parameterized as \mathbb{T}^2 .

After the previous machinery has been introduced, we will now comment on two specific results from the literature that are used in section 4.2 and Appendix B. First of all, from the *Uniformization theorem* of Schwarz and Klein (see section 4.4 from [141] for proof in modern language), every compact Riemann surface admits constant curvature metric. This is indeed useful, as from Gauss-Bonnet theorem we have

$$\int_{\Sigma_g} \sqrt{g_\Sigma} \mathcal{R}_\Sigma = \pi \chi(\Sigma_g) = 2\pi(1-g), \quad (\text{A.11})$$

in such cases we would have $\mathcal{R}_\Sigma = 2\pi(1-g) \text{vol}(\Sigma_g)^{-1}$. The question is now whether such metric (which results in an Einstein manifold, so solves the equation of motion in the vacuum) is dynamically reached. Indeed, Einstein-dilaton actions,

$$\int_{\Sigma_g} d^2x \sqrt{g_\Sigma} e^{-2\Phi} \{ \mathcal{R}_\Sigma + 4(\partial\Phi)^2 \}, \quad (\text{A.12})$$

feature a Ricci flow (see [142, 143] and references therein)

$$\partial_\sigma g_{mn} = -2(\mathcal{R}_{mn} + 2\nabla_m \partial_n \Phi), \quad \partial_\sigma \Phi = -\frac{1}{2}\mathcal{R}_\Sigma - \Delta\Phi, \quad (\text{A.13})$$

with σ some flow parameter, such that they eventually reach a constant curvature and dilaton configuration. This result no longer holds once extra ingredients, such as fluxes or backreacting branes are introducing, but it is safe to assume that if these are diluted or separated enough, most of the manifold will have an approximately constant scalar curvature.

Finally, we will introduce some machinery in order that we will use for flux potentials. Given a 1-form $F \in \Omega^1(\Sigma_g)$, we can expand it in both the dual and holomorphic basis as [113]

$$F = m^i \alpha_i + n^i \beta_i = u^i w_i + \bar{u}^i \bar{w}_i, \quad (\text{A.14})$$

modulo an exact form which is not relevant here. From (A.5) and (A.7) we find that the

different coefficients are related by

$$\begin{pmatrix} m \\ n \end{pmatrix} = \begin{pmatrix} \mathbb{I} & \mathbb{I} \\ \Omega & \bar{\Omega} \end{pmatrix} \begin{pmatrix} u \\ \bar{u} \end{pmatrix}. \quad (\text{A.15})$$

On the other hand, on the w basis the Hodge star acts as

$$\left. \begin{array}{l} \star w = -iw \\ \star \bar{w} = i\bar{w} \end{array} \right\} \implies \begin{pmatrix} \star u \\ \star \bar{u} \end{pmatrix} = \begin{pmatrix} -i\mathbb{I} & 0 \\ 0 & i\mathbb{I} \end{pmatrix} \begin{pmatrix} u \\ \bar{u} \end{pmatrix}. \quad (\text{A.16})$$

Finally, from (A.5), we are finally able to write the Hodge norm (which is precisely the induced flux potential) of F as

$$\|F\|^2 = \int_{\Sigma_g} F \wedge \star F = \begin{pmatrix} m & n \end{pmatrix} \mathbb{A} \begin{pmatrix} m \\ n \end{pmatrix}, \quad (\text{A.17})$$

with \mathbb{A} a $2g \times 2g$ real, positive definite symmetric matrix given by

$$\mathbb{A} = i \begin{pmatrix} 2\Omega(\Omega - \bar{\Omega})^{-1}\bar{\Omega} & -(\Omega + \bar{\Omega})(\Omega - \bar{\Omega})^{-1} \\ -(\Omega + \bar{\Omega})(\Omega - \bar{\Omega})^{-1} & 2(\Omega - \bar{\Omega})^{-1} \end{pmatrix}, \quad (\text{A.18})$$

where Ω is the period matrix.

B A quick overview of 1-cycle decay through tachyon condensation.

In this appendix we give some basic overview of handle decay in Riemann surfaces, i.e., $\Sigma_g \rightarrow \Sigma_{g-1}$ via tachyon condensation. For more details, see [113, 114]. We will work in the weak coupling and large volume limit ($g_s \ll 1$ and $\mathcal{V} \gg \ell_s^2$), so that string interactions and corrections can be safely ignored. As we will discuss later this section, this is the regime towards which a compactification on Σ_g with $g \geq 2$ naturally evolves. From (4.9), $\Omega_1^{\text{Spin}} = \langle \mathbb{S}_p^1 \rangle \simeq \mathbb{Z}_2$, so 1-cycles need anti-periodic boundary conditions in order to shrink them to nothing (otherwise a spin defect would need to be included²⁴).

As shown in Appendix A, Ricci flow results in Σ_g evolving towards having constant-curvature. For large volume, Gauss-Bonnet theorem implies $\alpha' \mathcal{R}_n = 2\pi(1-g) \frac{\alpha'}{\mathcal{V}} \ll 1$, so that we can consider the topology change locus neighborhood to be approximately flat, locally looking like a SUSY-breaking Scherk-Schwarz circle [62–64] of radius R with anti-periodic boundary conditions times a small interval, parameterized by $(\theta, r) \in \mathbb{S}^1 \times (r_0 - \epsilon, r_0 + \epsilon)$.

²⁴From [40], in type the IIA \mathbb{S}_p^1 class in Ω_1^{Spin} is killed through a $\mathbb{R}/\mathbb{Z}_2 \times \mathbb{S}_p^1$ defect consisting in an O8-plane wrapped along the circle (in the bulk, not in the boundary to nothing). For type IIB, the T-dual of the defect has a $(\mathbb{R} \times \mathbb{S}_p^1)/\mathbb{Z}_2$ geometry, with two O7-planes located at each end of the interval. These introduced defects are stringy by nature but, being located in the bulk of the bordism, should still allow for a smooth bordism to nothing after them.

The world-sheet energy of the n -th twisted sector is given by

$$\frac{m_n^2}{m_s^2} = -\frac{1}{2} + n^2 \frac{R^2}{\alpha'} , \quad (\text{B.1})$$

so that for $R < \sqrt{2\alpha'}$ the spectrum will have tachyonic states, resulting in an instability in the internal geometry. As shown in footnote 18, a flux potential automatically stabilizes the complex structure moduli at finite values, so $R < \sqrt{2\alpha'}$ is energetically obstructed (though as seen in section 4.2, topology changes are energetically favored, at least in the studied settings). As we will argue now, this tachyon condensation results in a barrier that prevents propagation through the $\mathbb{S}^1 \times (r_0 - \epsilon, r_0 + \epsilon)$ tube, effectively changing the topology of our internal geometry.

To do so, a (zero ghost picture) tachyon vertex is added to the $(1, 1)$ local world-sheet action,

$$S \supseteq \int d^2\sigma d\vartheta^+ d\vartheta^- T(X) , \quad \text{where} \quad T(X) = e^{k_0 X^0} \hat{T}(R) \cos(\omega \tilde{\Theta}) , \quad (\text{B.2})$$

with X^0 , R and $\tilde{\Theta}$ are the superspace coordinates associated to time t , radial direction r and the T-dual $\tilde{\theta}$ to θ [114], with $\hat{T}(R)$ complex as we have both winding and anti-winding modes in $T(X)$. It is further assumed that $\hat{T}(R)$ is localized at $r = r_0$, where the tube radius is the smallest, with an exponentially decaying profile in the r direction away from there. This results in a (classical) bosonic potential in the world-sheet action with the form

$$U(X) = (\partial T)^2 \left\{ \left[-k_0^2 \cos^2(\omega \tilde{\theta}) + \omega^2 \sin^2(\omega \tilde{\theta}) \right] \hat{T}(R)^2 + \cos^2(\omega \tilde{\theta}) (\partial_r \hat{T})^2 \right\} e^{2k_0 X^0} \quad (\text{B.3})$$

Now, for $\omega^2 \gg k_r^2 > k_0^2$, this results in a *classical* barrier for all values of $\tilde{\theta}$ and r over which \hat{T} has support, precisely when $\partial_r \hat{T}$ becomes significant. This prevents the different world-sheet modes from propagating along the tube, effectively disconnecting the two sides of the handle and changing the topology of the internal manifold. This qualitative behavior remains after quantum effects are considered, see sections 2 and 3 from [114].

As a final note, consider the following. Due to \hat{T} having a maximum at r_0 , $U(X)$ will have a minimum there (in general more, depending on the explicit shape of the profile), resulting in isolated vacua in which the Θ and R directions have been removed, with the resulting vacua being subcritical (this will result in additional bulk tachyons). This is evident from the invariance of the Witten index $\text{Tr}[(-1)^F e^{-\beta H}]$, which for supersymmetric sigma models such as this one is given by the Euler characteristic of the manifold our fields take values on. Now, as after the handle loss $\chi(\Sigma_{g-1}) = \chi(\Sigma_g) + 2$, then the new vacua will precisely have $n_F^{(0)} - n_B^{(0)} = 2$, as expected from the pair of bosonic d.o.f.'s lost.

References

- [1] S. Kachru, J. Pearson and H. L. Verlinde, *Brane / flux annihilation and the string dual of a nonsupersymmetric field theory*, *JHEP* **06** (2002) 021 [[hep-th/0112197](#)].
- [2] J. J. Blanco-Pillado, D. Schwartz-Perlov and A. Vilenkin, *Quantum Tunneling in Flux Compactifications*, *JCAP* **12** (2009) 006 [[0904.3106](#)].
- [3] M. Atiyah, J. M. Maldacena and C. Vafa, *An M theory flop as a large N duality*, *J. Math. Phys.* **42** (2001) 3209 [[hep-th/0011256](#)].
- [4] B. S. Acharya and S. Gukov, *M theory and singularities of exceptional holonomy manifolds*, *Phys. Rept.* **392** (2004) 121 [[hep-th/0409191](#)].
- [5] P. S. Aspinwall, B. R. Greene and D. R. Morrison, *Multiple mirror manifolds and topology change in string theory*, *Phys. Lett. B* **303** (1993) 249 [[hep-th/9301043](#)].
- [6] E. Witten, *Phases of N=2 theories in two-dimensions*, *Nucl. Phys. B* **403** (1993) 159 [[hep-th/9301042](#)].
- [7] A. Strominger, *Massless black holes and conifolds in string theory*, *Nucl. Phys. B* **451** (1995) 96 [[hep-th/9504090](#)].
- [8] B. R. Greene, D. R. Morrison and A. Strominger, *Black hole condensation and the unification of string vacua*, *Nucl. Phys.* **B451** (1995) 109 [[hep-th/9504145](#)].
- [9] S. B. Giddings and A. Strominger, *Axion Induced Topology Change in Quantum Gravity and String Theory*, *Nucl. Phys. B* **306** (1988) 890.
- [10] B. R. Greene and M. R. Plesser, *Duality in Calabi-Yau Moduli Space*, *Nucl. Phys. B* **338** (1990) 15.
- [11] A. Giveon, M. Porrati and E. Rabinovici, *Target space duality in string theory*, *Phys. Rept.* **244** (1994) 77 [[hep-th/9401139](#)].
- [12] E. Witten, *Anti-de Sitter space, thermal phase transition, and confinement in gauge theories*, *Adv. Theor. Math. Phys.* **2** (1998) 505 [[hep-th/9803131](#)].
- [13] I. n. García-Etxebarria and M. Montero, *Dai-Freed anomalies in particle physics*, *JHEP* **08** (2019) 003 [[1808.00009](#)].
- [14] S. Demulder, D. Lust and T. Raml, *Topology change and non-geometry at infinite distance*, *JHEP* **06** (2024) 079 [[2312.07674](#)].
- [15] E. Witten, *Instability of the Kaluza-Klein Vacuum*, *Nucl. Phys. B* **195** (1982) 481.
- [16] M. Fabinger and P. Horava, *Casimir effect between world branes in heterotic M theory*, *Nucl. Phys. B* **580** (2000) 243 [[hep-th/0002073](#)].
- [17] M. Dine, P. J. Fox and E. Gorbatov, *Catastrophic decays of compactified space-times*, *JHEP* **09** (2004) 037 [[hep-th/0405190](#)].
- [18] G. T. Horowitz, J. Orgera and J. Polchinski, *Nonperturbative Instability of AdS(5) x S**5/Z(k)*, *Phys. Rev. D* **77** (2008) 024004 [[0709.4262](#)].
- [19] I.-S. Yang, *Stretched extra dimensions and bubbles of nothing in a toy model landscape*, *Phys. Rev. D* **81** (2010) 125020 [[0910.1397](#)].

- [20] J. J. Blanco-Pillado and B. Shlaer, *Bubbles of Nothing in Flux Compactifications*, *Phys. Rev. D* **82** (2010) 086015 [[1002.4408](#)].
- [21] J. J. Blanco-Pillado, H. S. Ramadhan and B. Shlaer, *Decay of flux vacua to nothing*, *JCAP* **10** (2010) 029 [[1009.0753](#)].
- [22] A. R. Brown and A. Dahlen, *Bubbles of Nothing and the Fastest Decay in the Landscape*, *Phys. Rev. D* **84** (2011) 043518 [[1010.5240](#)].
- [23] J. J. Blanco-Pillado, H. S. Ramadhan and B. Shlaer, *Bubbles from Nothing*, *JCAP* **01** (2012) 045 [[1104.5229](#)].
- [24] A. R. Brown and A. Dahlen, *On 'nothing' as an infinitely negatively curved spacetime*, *Phys. Rev. D* **85** (2012) 104026 [[1111.0301](#)].
- [25] S. de Alwis, R. Gupta, E. Hatefi and F. Quevedo, *Stability, Tunneling and Flux Changing de Sitter Transitions in the Large Volume String Scenario*, *JHEP* **11** (2013) 179 [[1308.1222](#)].
- [26] A. R. Brown, *Decay of hot Kaluza-Klein space*, *Phys. Rev. D* **90** (2014) 104017 [[1408.5903](#)].
- [27] J. J. Blanco-Pillado, B. Shlaer, K. Sousa and J. Urrestilla, *Bubbles of Nothing and Supersymmetric Compactifications*, *JCAP* **10** (2016) 002 [[1606.03095](#)].
- [28] H. Ooguri and L. Spodyneiko, *New Kaluza-Klein instantons and the decay of AdS vacua*, *Phys. Rev. D* **96** (2017) 026016 [[1703.03105](#)].
- [29] G. Dibitetto, N. Petri and M. Schillo, *Nothing really matters*, *JHEP* **08** (2020) 040 [[2002.01764](#)].
- [30] I. García Etxebarria, M. Montero, K. Sousa and I. Valenzuela, *Nothing is certain in string compactifications*, *JHEP* **12** (2020) 032 [[2005.06494](#)].
- [31] P. Bomans, D. Cassani, G. Dibitetto and N. Petri, *Bubble instability of mIIA on $\text{AdS}_4 \times S^6$* , *SciPost Phys.* **12** (2022) 099 [[2110.08276](#)].
- [32] P. Draper, I. G. Garcia and B. Lillard, *Bubble of nothing decays of unstable theories*, *Phys. Rev. D* **104** (2021) L121701 [[2105.08068](#)].
- [33] P. Draper, I. Garcia Garcia and B. Lillard, *De Sitter decays to infinity*, *JHEP* **12** (2021) 154 [[2105.10507](#)].
- [34] N. Petri, *Bubbles of nothing and AdS instabilities*, *PoS CORFU2021* (2022) 170 [[2205.00884](#)].
- [35] I. Bandos, J. J. Blanco-Pillado, K. Sousa and M. A. Urkiola, *Brane nucleation in supersymmetric models*, *JHEP* **10** (2023) 061 [[2306.09412](#)].
- [36] Y. Ookouchi, R. Sato and S. Tsukahara, *Decay of Kaluza-Klein Vacuum via Singular Instanton*, [2404.13917](#).
- [37] J. J. Heckman and M. Hübner, *Celestial Topology, Symmetry Theories, and Evidence for a Non-SUSY D3-Brane CFT*, [2406.08485](#).
- [38] P. Horava and E. Witten, *Heterotic and type I string dynamics from eleven-dimensions*, *Nucl. Phys. B* **460** (1996) 506 [[hep-th/9510209](#)].
- [39] P. Horava and E. Witten, *Eleven-dimensional supergravity on a manifold with boundary*, *Nucl. Phys. B* **475** (1996) 94 [[hep-th/9603142](#)].

- [40] J. McNamara and C. Vafa, *Cobordism Classes and the Swampland*, [1909.10355](#).
- [41] C. Vafa, *The String landscape and the swampland*, [hep-th/0509212](#).
- [42] T. D. Brennan, F. Carta and C. Vafa, *The String Landscape, the Swampland, and the Missing Corner*, *PoS TASI2017* (2017) 015 [[1711.00864](#)].
- [43] E. Palti, *The Swampland: Introduction and Review*, *Fortsch. Phys.* **67** (2019) 1900037 [[1903.06239](#)].
- [44] M. van Beest, J. Calderón-Infante, D. Mirfendereski and I. Valenzuela, *Lectures on the Swampland Program in String Compactifications*, *Phys. Rept.* **989** (2022) 1 [[2102.01111](#)].
- [45] M. Graña and A. Herráez, *The Swampland Conjectures: A Bridge from Quantum Gravity to Particle Physics*, *Universe* **7** (2021) 273 [[2107.00087](#)].
- [46] D. Harlow, B. Heidenreich, M. Reece and T. Rudelius, *Weak gravity conjecture*, *Rev. Mod. Phys.* **95** (2023) 035003 [[2201.08380](#)].
- [47] N. B. Agmon, A. Bedroya, M. J. Kang and C. Vafa, *Lectures on the string landscape and the Swampland*, [2212.06187](#).
- [48] T. Banks and L. J. Dixon, *Constraints on String Vacua with Space-Time Supersymmetry*, *Nucl. Phys.* **B307** (1988) 93.
- [49] R. Kallosh, A. D. Linde, D. A. Linde and L. Susskind, *Gravity and global symmetries*, *Phys.Rev.* **D52** (1995) 912 [[hep-th/9502069](#)].
- [50] T. Banks and N. Seiberg, *Symmetries and Strings in Field Theory and Gravity*, *Phys. Rev.* **D83** (2011) 084019 [[1011.5120](#)].
- [51] M. Montero and C. Vafa, *Cobordism Conjecture, Anomalies, and the String Lamppost Principle*, *JHEP* **01** (2021) 063 [[2008.11729](#)].
- [52] M. Dierigl, J. J. Heckman, M. Montero and E. Torres, *IIB string theory explored: Reflection 7-branes*, *Phys. Rev. D* **107** (2023) 086015 [[2212.05077](#)].
- [53] S. R. Coleman, *The Fate of the False Vacuum. 1. Semiclassical Theory*, *Phys. Rev. D* **15** (1977) 2929.
- [54] E. Witten, *Supersymmetry and Morse theory*, *J. Diff. Geom.* **17** (1982) 661.
- [55] R. D. Sorkin, *CONSEQUENCES OF SPACE-TIME TOPOLOGY*, .
- [56] J. Louko and R. D. Sorkin, *Complex actions in two-dimensional topology change*, *Class. Quant. Grav.* **14** (1997) 179 [[gr-qc/9511023](#)].
- [57] H. F. Dowker and R. S. Garcia, *A Handlebody calculus for topology change*, *Class. Quant. Grav.* **15** (1998) 1859 [[gr-qc/9711042](#)].
- [58] F. Dowker and S. Surya, *Topology change and causal continuity*, *Phys. Rev. D* **58** (1998) 124019 [[gr-qc/9711070](#)].
- [59] H. F. Dowker, R. S. Garcia and S. Surya, *Morse index and causal continuity: A Criterion for topology change in quantum gravity*, *Class. Quant. Grav.* **17** (2000) 697 [[gr-qc/9910034](#)].
- [60] L. García-Heveling, *Topology change with Morse functions: progress on the Borde–Sorkin conjecture*, *Adv. Theor. Math. Phys.* **27** (2023) 1159 [[2202.09833](#)].

- [61] S. Lüst, *An index for flux vacua*, [2405.04584](#).
- [62] J. Scherk and J. H. Schwarz, *Spontaneous Breaking of Supersymmetry Through Dimensional Reduction*, *Phys. Lett. B* **82** (1979) 60.
- [63] J. Scherk and J. H. Schwarz, *How to Get Masses from Extra Dimensions*, *Nucl. Phys. B* **153** (1979) 61.
- [64] C. Kounnas and B. Rostand, *Coordinate Dependent Compactifications and Discrete Symmetries*, *Nucl. Phys. B* **341** (1990) 641.
- [65] R. Schon and S.-T. Yau, *On the Proof of the positive mass conjecture in general relativity*, *Commun. Math. Phys.* **65** (1979) 45.
- [66] E. Witten, *A Simple Proof of the Positive Energy Theorem*, *Commun. Math. Phys.* **80** (1981) 381.
- [67] D. W. Anderson, E. H. Brown and F. P. Peterson, *The structure of the spin cobordism ring*, *Annals of Mathematics* **86** (1967) 271.
- [68] I. García-Etxebarria, M. Montero and A. M. Uranga, *Closed tachyon solitons in type II string theory*, *Fortsch. Phys.* **63** (2015) 571 [[1505.05510](#)].
- [69] Z. Wan and J. Wang, *Higher anomalies, higher symmetries, and cobordisms I: classification of higher-symmetry-protected topological states and their boundary fermionic/bosonic anomalies via a generalized cobordism theory*, *Ann. Math. Sci. Appl.* **4** (2019) 107 [[1812.11967](#)].
- [70] T. Hertog, G. T. Horowitz and K. Maeda, *Negative energy density in Calabi-Yau compactifications*, *JHEP* **05** (2003) 060 [[hep-th/0304199](#)].
- [71] T. Hertog, G. T. Horowitz and K. Maeda, *Negative energy in string theory and cosmic censorship violation*, *Phys. Rev. D* **69** (2004) 105001 [[hep-th/0310054](#)].
- [72] E. Curiel, *A Primer on Energy Conditions*, *Einstein Stud.* **13** (2017) 43 [[1405.0403](#)].
- [73] P. Draper, B. Lillard and C. Skye, *Neutralizing topological obstructions to bubbles of nothing*, *JHEP* **10** (2023) 049 [[2305.17838](#)].
- [74] J. J. Blanco-Pillado, J. R. Espinosa, J. Huertas and K. Sousa, *Tunneling potentials to nothing*, *Phys. Rev. D* **109** (2024) 084057 [[2311.18821](#)].
- [75] J. J. Blanco-Pillado, J. R. Espinosa, J. Huertas and K. Sousa, *Bubbles of nothing: the tunneling potential approach*, *JCAP* **03** (2024) 029 [[2312.00133](#)].
- [76] M. Delgado, *The bubble of nothing under T-duality*, *JHEP* **05** (2024) 333 [[2312.09291](#)].
- [77] B. Friedrich and A. Hebecker, *The boundary proposal*, *Phys. Lett. B* **856** (2024) 138946 [[2403.18892](#)].
- [78] R. Angius, J. Calderón-Infante, M. Delgado, J. Huertas and A. M. Uranga, *At the end of the world: Local Dynamical Cobordism*, *JHEP* **06** (2022) 142 [[2203.11240](#)].
- [79] B. Friedrich, A. Hebecker and J. Walcher, *Cobordism and bubbles of anything in the string landscape*, *JHEP* **02** (2024) 127 [[2310.06021](#)].
- [80] A. Vilenkin, *Cosmic Strings and Domain Walls*, *Phys. Rept.* **121** (1985) 263.
- [81] D. Garfinkle, *General Relativistic Strings*, *Phys. Rev. D* **32** (1985) 1323.

- [82] E. Dudas and J. Mourad, *Brane solutions in strings with broken supersymmetry and dilaton tadpoles*, *Phys. Lett. B* **486** (2000) 172 [[hep-th/0004165](#)].
- [83] E. Dudas, J. Mourad and C. Timirgaziu, *Time and space dependent backgrounds from non-supersymmetric strings*, *Nucl. Phys. B* **660** (2003) 3 [[hep-th/0209176](#)].
- [84] E. Dudas, G. Pradisi, M. Nicolosi and A. Sagnotti, *On tadpoles and vacuum redefinitions in string theory*, *Nucl. Phys. B* **708** (2005) 3 [[hep-th/0410101](#)].
- [85] I. Basile, J. Mourad and A. Sagnotti, *On Classical Stability with Broken Supersymmetry*, *JHEP* **01** (2019) 174 [[1811.11448](#)].
- [86] R. Antonelli and I. Basile, *Brane annihilation in non-supersymmetric strings*, *JHEP* **11** (2019) 021 [[1908.04352](#)].
- [87] I. Basile, *Supersymmetry breaking, brane dynamics and Swampland conjectures*, *JHEP* **10** (2021) 080 [[2106.04574](#)].
- [88] J. Mourad and A. Sagnotti, *On warped string vacuum profiles and cosmologies. Part I. Supersymmetric strings*, *JHEP* **12** (2021) 137 [[2109.06852](#)].
- [89] J. Mourad and A. Sagnotti, *On warped string vacuum profiles and cosmologies. Part II. Non-supersymmetric strings*, *JHEP* **12** (2021) 138 [[2109.12328](#)].
- [90] G. Buratti, M. Delgado and A. M. Uranga, *Dynamical tadpoles, stringy cobordism, and the SM from spontaneous compactification*, *JHEP* **06** (2021) 170 [[2104.02091](#)].
- [91] G. Buratti, J. Calderón-Infante, M. Delgado and A. M. Uranga, *Dynamical Cobordism and Swampland Distance Conjectures*, *JHEP* **10** (2021) 037 [[2107.09098](#)].
- [92] R. Angius, M. Delgado and A. M. Uranga, *Dynamical Cobordism and the beginning of time: supercritical strings and tachyon condensation*, *JHEP* **08** (2022) 285 [[2207.13108](#)].
- [93] R. Blumenhagen, N. Cribiori, C. Kneissl and A. Makridou, *Dynamical cobordism of a domain wall and its companion defect 7-brane*, *JHEP* **08** (2022) 204 [[2205.09782](#)].
- [94] I. Basile, S. Raucci and S. Thomée, *Revisiting Dudas-Mourad Compactifications*, *Universe* **8** (2022) 544 [[2209.10553](#)].
- [95] R. Blumenhagen, C. Kneissl and C. Wang, *Dynamical Cobordism Conjecture: solutions for end-of-the-world branes*, *JHEP* **05** (2023) 123 [[2303.03423](#)].
- [96] R. Angius, J. Huertas and A. M. Uranga, *Small black hole explosions*, *JHEP* **06** (2023) 070 [[2303.15903](#)].
- [97] J. Huertas and A. M. Uranga, *Aspects of dynamical cobordism in AdS/CFT*, *JHEP* **08** (2023) 140 [[2306.07335](#)].
- [98] R. Angius, A. Makridou and A. M. Uranga, *Intersecting end of the world branes*, *JHEP* **03** (2024) 110 [[2312.16286](#)].
- [99] I. n. García Etxebarria, J. Huertas and A. M. Uranga, *SymTFT Fans: The Symmetry Theory of 4d $N=4$ Super Yang-Mills on spaces with boundaries*, [2409.02156](#).
- [100] J. Huertas and A. M. Uranga, *End of the World Brane Dynamics in Holographic 4d $N = 4$ $SU(N)$ with 3d $N = 2$ Boundary Conditions*, [2410.05368](#).

- [101] R. Angius, A. M. Uranga and C. Wang, *End of the World Boundaries for Chiral Quantum Gravity Theories*, [2410.07322](#).
- [102] R. Angius, *End of The World brane networks for infinite distance limits in CY moduli space*, [2404.14486](#).
- [103] R. Thom, *Quelques propriétés globales des variétés différentiables*, *Commentarii Mathematici Helvetici* **28** (1954) 17.
- [104] A. Putman, *Half lives, half dies and the signature of boundaries*, November, 2022.
- [105] R. Orita, *Morse–bott inequalities for manifolds with boundary*, *Tokyo Journal of Mathematics* **41** (2018) .
- [106] E. Pitcher, *Inequalities of critical point theory.*, *Bull. Am. Math. Soc.* **64** (1958) 1.
- [107] A. Debray, M. Dierigl, J. J. Heckman and M. Montero, *The Chronicles of IIBordia: Dualities, Bordisms, and the Swampland*, [2302.00007](#).
- [108] L. E. Ibáñez and A. M. Uranga, *String theory and particle physics: An introduction to string phenomenology*. Cambridge University Press, 2012.
- [109] T. Van Riet and G. Zoccarato, *Beginners lectures on flux compactifications and related Swampland topics*, *Phys. Rept.* **1049** (2024) 1 [[2305.01722](#)].
- [110] Y. Tachikawa and K. Yonekura, *Why are fractional charges of orientifolds compatible with Dirac quantization?*, *SciPost Phys.* **7** (2019) 058 [[1805.02772](#)].
- [111] T. Pantev and E. Sharpe, *Duality group actions on fermions*, *JHEP* **11** (2016) 171 [[1609.00011](#)].
- [112] A. Debray, M. Dierigl, J. J. Heckman and M. Montero, *The anomaly that was not meant IIB*, [2107.14227](#).
- [113] A. Saltman and E. Silverstein, *A New handle on de Sitter compactifications*, *JHEP* **01** (2006) 139 [[hep-th/0411271](#)].
- [114] A. Adams, X. Liu, J. McGreevy, A. Saltman and E. Silverstein, *Things fall apart: Topology change from winding tachyons*, *JHEP* **10** (2005) 033 [[hep-th/0502021](#)].
- [115] M. Billò, M. Frau, F. Fucito, L. Gallot, A. Lerda and J. F. Morales, *On the $D(-1)/D7$ -brane systems*, *JHEP* **04** (2021) 096 [[2101.01732](#)].
- [116] S. Reymond, M. Trigiante and T. Van Riet, *Supergravity solutions for Dp - $D(6 - p)$ bound states: from $p = 7$ to $p = -1$* , [2410.02616](#).
- [117] R. Blumenhagen, D. Lüst and S. Theisen, *Basic concepts of string theory*, Theoretical and Mathematical Physics. Springer, Heidelberg, Germany, 2013, [10.1007/978-3-642-29497-6](#).
- [118] M. P. Dabrowski, J. Garecki and D. B. Blaschke, *Conformal transformations and conformal invariance in gravitation*, *Annalen Phys.* **18** (2009) 13 [[0806.2683](#)].
- [119] A. Scorpan, *The wild world of 4-manifolds*, 2005, <https://api.semanticscholar.org/CorpusID:117823549>.
- [120] D. J. Gross and M. J. Perry, *Magnetic Monopoles in Kaluza-Klein Theories*, *Nucl. Phys. B* **226** (1983) 29.
- [121] R. D. Sorkin, *Kaluza-Klein Monopole*, *Phys. Rev. Lett.* **51** (1983) 87.

- [122] E. Witten, *The "Parity" Anomaly On An Unorientable Manifold*, *Phys. Rev. B* **94** (2016) 195150 [[1605.02391](#)].
- [123] K. Dasgupta and S. Mukhi, *Orbifolds of M theory*, *Nucl. Phys. B* **465** (1996) 399 [[hep-th/9512196](#)].
- [124] E. Witten, *Five-branes and M-theory on an orbifold*, *Nucl. Phys. B* **463** (1996) 383 [[hep-th/9512219](#)].
- [125] F. Hirzebruch, *über eine klasse von einfach-zusammenhängenden komplexen mannigfaltigkeiten.*, *Mathematische Annalen* **124** (1951) 77.
- [126] A. Suciuc, *Homology 4-spheres with distinct k-invariants*, *Topology and its Applications* **25** (1987) 103.
- [127] G. T. Horowitz and K. Maeda, *Colliding Kaluza-Klein bubbles*, *Class. Quant. Grav.* **19** (2002) 5543 [[hep-th/0207270](#)].
- [128] B. Freivogel, G. T. Horowitz and S. Shenker, *Colliding with a crunching bubble*, *JHEP* **05** (2007) 090 [[hep-th/0703146](#)].
- [129] M. Kleban, *Cosmic Bubble Collisions*, *Class. Quant. Grav.* **28** (2011) 204008 [[1107.2593](#)].
- [130] J. Moritz and I. Valenzuela, *to appear*, .
- [131] M. Atiyah, *Topological quantum field theories*, *Inst. Hautes Etudes Sci. Publ. Math.* **68** (1989) 175.
- [132] J. Lurie, *On the classification of topological field theories*, 2009.
- [133] S. W. Hawking and N. Turok, *Open inflation without false vacua*, *Phys. Lett. B* **425** (1998) 25 [[hep-th/9802030](#)].
- [134] N. Turok and S. W. Hawking, *Open inflation, the four form and the cosmological constant*, *Phys. Lett. B* **432** (1998) 271 [[hep-th/9803156](#)].
- [135] J. Garriga, *Smooth 'creation' of an open universe in five-dimensions*, [hep-th/9804106](#).
- [136] R. Bousso and A. Chamblin, *Open inflation from nonsingular instantons: Wrapping the universe with a membrane*, *Phys. Rev. D* **59** (1999) 063504 [[hep-th/9805167](#)].
- [137] M. Dierigl, J. J. Heckman, M. Montero and E. Torres, *R7-branes as charge conjugation operators*, *Phys. Rev. D* **109** (2024) 046004 [[2305.05689](#)].
- [138] A. Strominger, S.-T. Yau and E. Zaslow, *Mirror symmetry is T duality*, *Nucl. Phys. B* **479** (1996) 243 [[hep-th/9606040](#)].
- [139] K. Chan, *The Strominger-Yau-Zaslow conjecture and its impact*, *arXiv preprint arXiv:1408.6062* (2014) .
- [140] B. S. Acharya, *Supersymmetry, Ricci Flat Manifolds and the String Landscape*, *JHEP* **08** (2020) 128 [[1906.06886](#)].
- [141] J. Jost, *Compact Riemann Surfaces: An Introduction to Contemporary Mathematics*, Springer Universitext. 12, 2006.
- [142] G. Perelman, *The Entropy formula for the Ricci flow and its geometric applications*, [math/0211159](#).

- [143] D. M. Velázquez, D. De Biasio and D. Lust, *Cobordism, singularities and the Ricci flow conjecture*, *JHEP* **01** (2023) 126 [[2209.10297](#)].